CHAPTER – 3A

Building the framework from pentahelicenes: Synthesis and study of pyrrolo[7]helicene with unsymmetrical scaffold

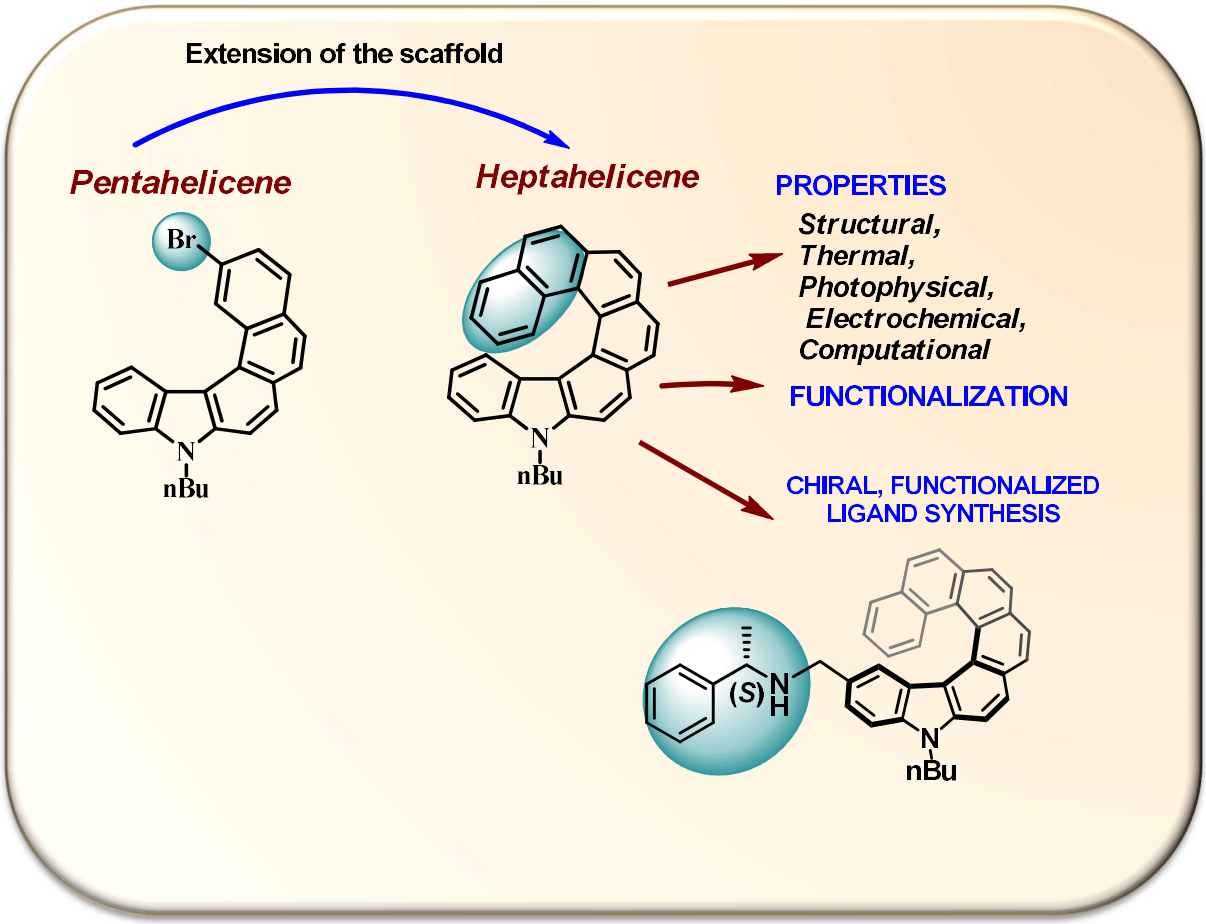

Table of Contents

3.1.1 Introduction

In our work on the study of five-membered helical molecules it was clear that unless an attachment was made in the fjord region of the helical core, the stability of the enantiomers was compromised at ambient temperatures rendering conformationally labile isomers of helicenes. However, this is not the case for higher order helicenes (n>6), which comprises of a very stable helical scaffold with greater racemization barriers and most significantly exhibit modified properties due to the extension of the helical framework. Hence, various strategies have been developed and explored to synthesize higher order helical moleucules.

One of the popular strategies to build helicenes of higher order is by extending the pre-existing skeletons, for instance in the year 1999, Katz and group synthesized optically pure [8]helicene derivative from nonracemic [6]helicenebisquinone and 1,2-phenylenediamine. [1] The strategy employed to extend the helical core was by the addition of *ortho*-fused rings at terminal ends as shown in scheme 3.1.1. This was made possible by two realizations. One is that, in the presence of $Cu(OAc)_2$, secondary amines add to [6]helicenebisquinone **1** to produce adducts specifically of structure **2**. The other discovery is that 1,2-phenylenediamine combines with 1,4-naphthoquinone in acetic acid to give 5-hydroxybenzo[*a*]phenazine, a transformation that fuses a quinoxaline to the naphthalene core. An analogous reaction with bisquinone **1** would fuse two such rings to the [6]helicene. Moreover, if it occurred with the same regioselectivity, simple reagents should convert a derivative of [6]helicene that is itself easy to obtain into a derivative of [8]helicene. Since bisquinone **1** can be obtained optically pure, any [8]helicene made from it would be too. Hence, using this strategy optically pure [8]helicene was synthesized.

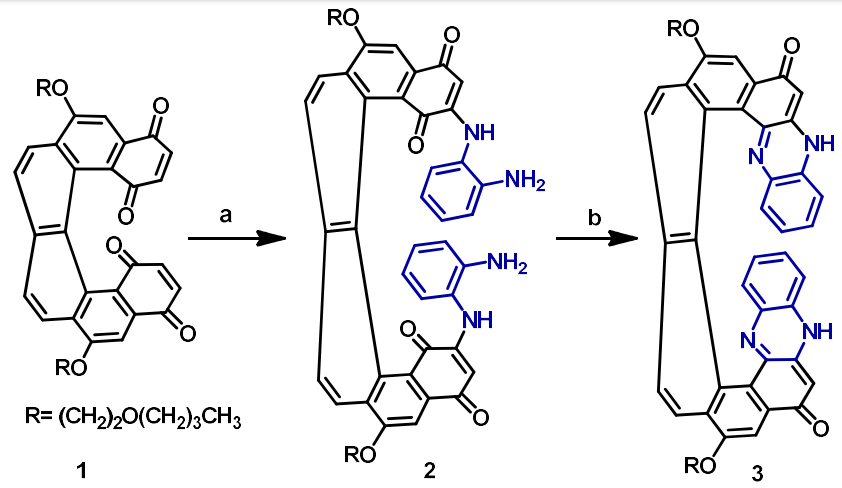

(a) 1,2-phenylenediamine, $Cu(OAc)_2$, 1:1 MeOH-CH_2Cl_2, 2.5h (b) AcOH, reflux, 2.5h

Scheme 3.1.1 : Conversion of [6]helicene into an [8]helicene

Further, the optically pure [8]helicene derivative **3**, was then converted into the orthoquinone **5** by combining with benzeneseleninic anhydride which in turn reacts with ethylenediamine to form a helical bis-bidentate ligand **6**. As shown in scheme 2, ethylenediamine, a reagent that converts 9, 10-phenanthrenequinone into dibenzo[*f*,*h*]quinoxaline, also converts **5** into **6** in 48% yield. This bidentate ligand was then complexed with Re metal. Compound **6** reacts with Re-$(CO)_5Cl$ in toluene to give compound **7**, which was isolated in 30% yield. Rhenium complex **7** is a red solid that does not melt at temperatures below 220 °C, and it is soluble in CH_2Cl_2, $CHCl_3$, toluene, and THF. The ^1H NMR spectrum showed that its structure is symmetrical and its IR spectrum has the three absorptions required of the metal carbonyls at 2023, 1926, and 1893 cm^{-1}.

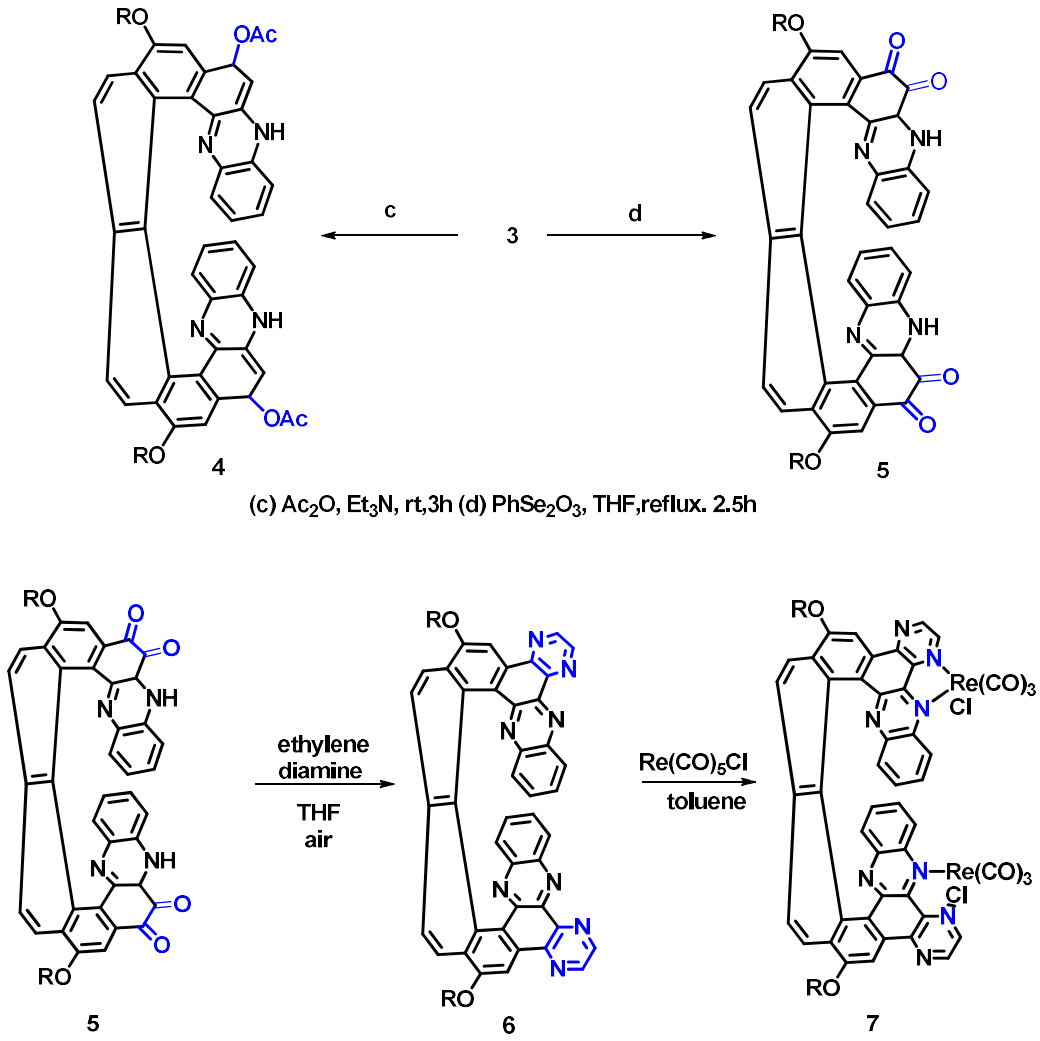

Scheme 3.1.2: Synthesis of Re-complex of [8]helicene

Another approach for the synthesis of novel, functionalized, helicene-like quinones and bisquinones was based on the organometallic route by chromium-templated [3+2+1] benzannulation reaction of fischer type carbene complexes.[2] This strategy provides a non-photochemical access to a broad series of helical scaffolds bearing five, six and seven *ortho*-fused carbo- or heterocycles. The syntheses are based on a progressive mono- and bidirectional chromium-templated [3+2+1] benzannulation of racemic (sila)ketal-tethered binaphthyl carbene complexes with various alkynes. As shown in scheme 3, di-tert-butyldichlorosilane and dichlorodiphenylmethane were first used for the incorporation of of one metal carbene moiety to study the feasibility of monobenzannulation. A single metal-halogen exchange in racemic **8** and **9** was carried out with 1.1 equivalents of *n*-butyllithium followed by addition of hexacarbonyl chromium to afford the pentacarbonyl acyl chromate which was subjected to *O*-alkylation with trimethyloxonium tetrafluroborate to render helical carbene complexes **10** and **11**.

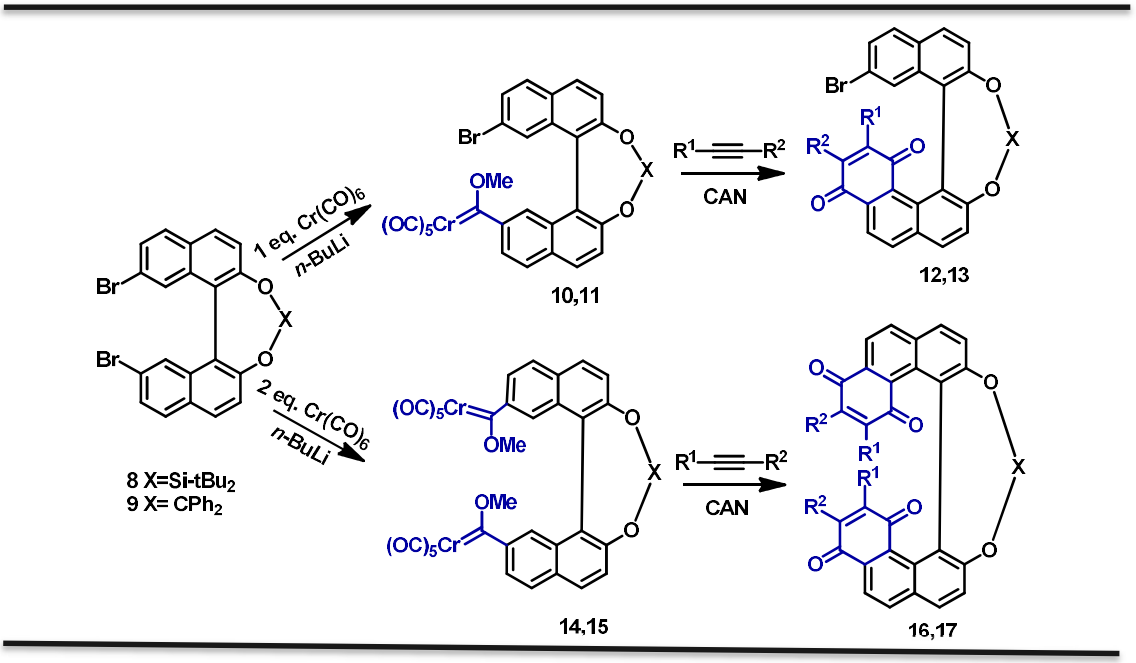

***Scheme 3.1.3**: [6]- and [7]helicene-like quinones via mono- and bidirectional chromium-templated benzannulation strategy*

The helical carbene complex was then subjected to a typical angular [3+2+1] benzannulation with various alkynes in dichloromethane at 55 °C to yield the substituted [6]helicene-like quinones in moderate yields after oxidative work-up with ceric ammonium nitrate (CAN). Using the similar route with 2 equivalents of hexacarbonyl chromium, a biscarbene complex was formed which was further subjected to bidirectional benzannulation to further extend the helical bisquinones.

The benzannulation strategy was also applied for the synthesis of functionalized heterohelicenes by the same research group.[3] A series of oxa and thia heterohelicenes was accessed by chromium-templated [3+2+1] benzannulation reaction of hetero[5]helicene carbene complexes. As in the previous study, they first focused on the incorporation of one chromium carbene moiety to probe the feasibility of monobenzannulation. Thus, reaction of the respective monolithiated hetero[5]helicene with hexacarbonyl chromium yielded the desired pentacarbonyl acyl chromate which underwent O-alkylation with Meerwein's reagent to give methoxycarbene complexes which then underwent the typical angular [3+2+1] benzannulation with various alkynes in dichloromethane to yield substituted hetero[6]helicene quinone **20**. However, for the synthesis of the racemic biscarbene complexes by depicted Fischer route using two equivalents of the respective reagents, bimetalated heterohelicenes along with mono-metalated byproducts were formed. The problem of incomplete biscarbene functionalization has been previously reported for other heteroarenes. The bis-carbene complexes of the oxa counterpart on benzannulation afforded the bisquinones via bisangular appending mode but the thia counterpart underwent divergent bidirectional benzannulation affording two bis-quinonoid products.

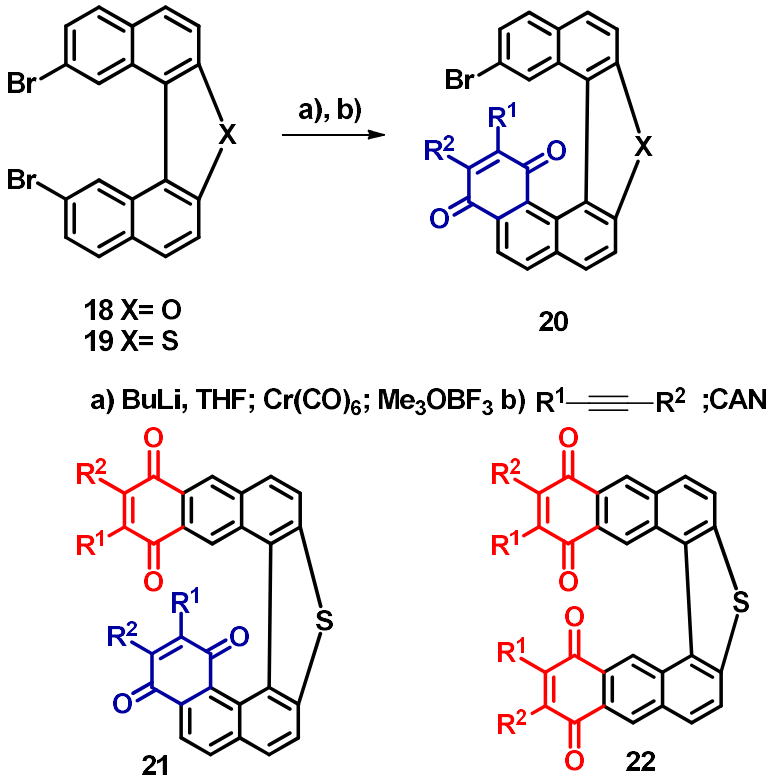

Scheme 3.1.4: Benzannulation strategy for the synthesis of heterohelicenes

Extending the protocol of synthesizing higher order helicenes from preexisting helical scaffolds, a previous work from our group involves the synthesis of oxa[11]helicene from [5]helicene.[4] The heterohelicene was synthesized by reactions involving oxidative coupling and dehydrative cyclization. The precursor **23** was synthesized from its corresponding triol derivative by acid-catalyzed ether formation using p-toluenesulfonic acid in toluene. The oxidative homo-coupling of 2-hydroxy-7-oxa[5]helicene was the key step in the synthesis of the target [11]helicene.

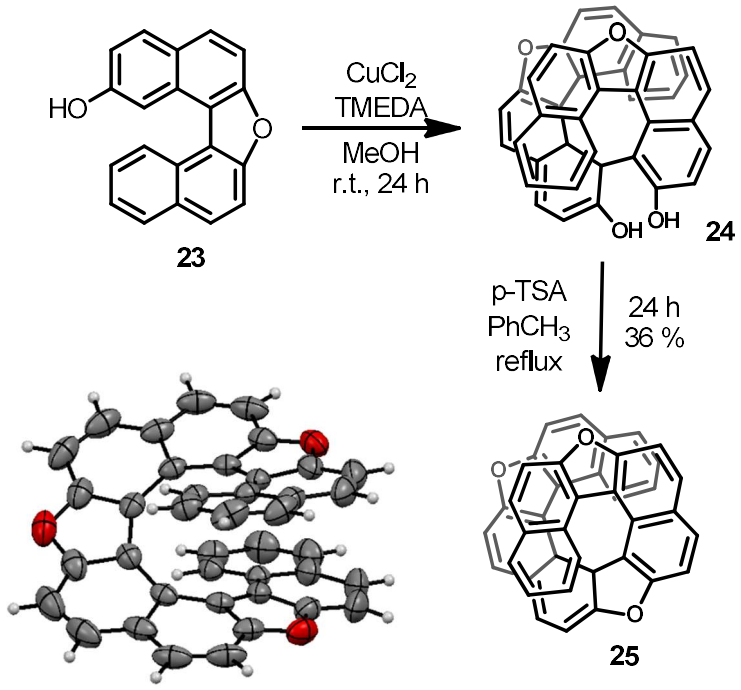

***Scheme 3.1.4**: Synthesis of trioxa[11]helicene from oxa[5]helicene core*

As we were already acquainted with the chemistry of pentahelicenes, we thought of utilizing the five membered helicene and extend it to synthesize seven membered hetero helicene. Moreover, so far there are several reports for the synthesis of symmetrical scaffolds of heptahelicenes but very few reports on the unsymmetrical scaffolds. So, we decided to explore the chemistry of seven-membered hetero helicenes utilizing a pentahelicene core with an unsymmetrical scaffold.

In 2015, Liu and group[5] reported the synthesis of monoaza[6]helicene having an unsymmetrical helical scaffold and studied its application as organic light-emitting diodes. It is well known that helical molecular geometry is effective in blocking the π-conjugation and decrease the close packing of molecules thus increasing its utility in optical devices. The doped OLED based on this unsymmetrical [6]helicene was the first example of helicene that exhibited a brightness of more than 3000 cd m^{-2} with high colour purity. Intrigued by this study of unsymmetrical aza[7]helicene and combining the extension strategy, we thought of synthesizing an unsymmetrical heptahelicene from a pre-existing scaffold.

3.1.2 Results and discussion

In order to develop a strategy to elongate helicene from a pre-existing skeleton, we need to fulfil three basic requirements. First is the size of the basic helical skeleton on which we would build the system. Second is the position of the functional group on the pre-existing skeleton and third is the functionality required to aid in extension. Our first target was to choose a suitable helical scaffold for extension and for this study we thought to opt for a helical skeleton with five-membered rings as we had a better understanding of the system from our studies on pentacyclic helicenes. Moreover, it would be easy to synthesize a pentahelical skeleton with direction of cyclization in angular mode, as the five-membered scaffold as such does not pose a challenge for linear cyclization due to low steric hindrance. As for the second criteria that is the position of the functional group, it is clear from our study with pentacyclic systems that even a methyl moiety at C-1 position of a five-membered helicene raised the steric hindrance to a considerable degree which may lead to the formation of linearly cyclized system which will be inadequate for further helical extension. Thus, it would be necessary to install the substituent at C-2 position. Now to build the helicene, functional groups like bromo, methoxy or hydroxyl substituents are versatile for various chemical transformations. A literature review of similar helicenes fulfilling all these basic requirements led us to the work of Ben Hassine and group. In 2013, they had reported a new helically chiral bromo functionalized pentacyclic system containing one pyrrole ring.[6] The synthesis was high yielding with exclusive formation of the angularly cyclized product. (Scheme 3.1.5)

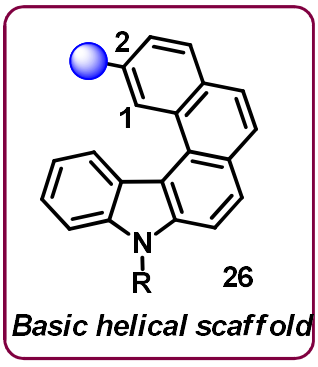

Basic helical scaffold

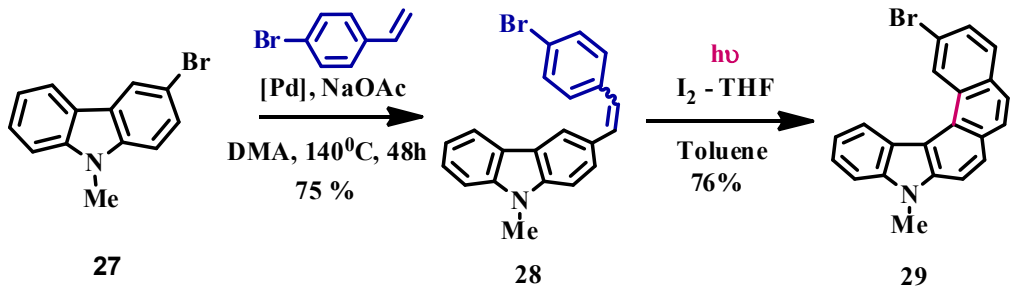

Scheme 3.1.5: Synthesis of C-2 substituted pentahelicene by Ben Hassine and group

3.1.2.1 *Synthesis of the helical precursor for extension*

The synthesis of 2-bromoaza[5]helicene was carried out with the *N*-butylation of carbazole. To introduce the n-butyl group in the side-chain, carbazole was treated with 1-bromobutane in presence of KOH as base. The product exhibited good solubility and was eluted in petroleum ether. *N*-butylated carbazole was then subjected to Vilsmeier-Haack formylation (under monoformylation conditions) using standard reagents of dimethyl formamide and phosphorous oxychloride, which progressed with good yield (~75%). Formylation was selective at the *para*- position to the nitrogen atom of carbazole and 9-butyl-3-formyl carbazole was obtained as the only product. 9-butyl-3-formyl carbazole **30** was then subjected to Wittig reaction with 4-bromobenzyltriphenylphosphonium bromide in dry methanol using sodium methoxide as base, the reaction progressed efficiently resulting in the precipitation of a pale-yellow solid. Purification of Wittig reaction product **31** was done using column chromatography giving good yield (81%). The Wittig olefin **31** was subjected to standard photocyclization conditions using iodine and tetrahydrofuran (acid scavenger) in toluene as solvent, careful monitoring (by TLC) and analysis of the product indicated the formation of helicene within 12 hours. The reaction was carried out in immersion well photo reactor using 250 W High Pressure Mercury Vapour Lamp (HPMVL) resulting in good yield of 9-butyl-2-bromo aza[5]helicene **32** (72%)

The formation of the bromosubstituted pentahelicene was confirmed from the ^{1}H-NMR analysis which showed the disappearance of the trans-olefinic signals at δ7.1 and 7.4 ppm. Moreover, after angular mode of cyclization, the proton next to the bromo-substituted carbon experiences de-shielding due to the ring current effect and appears downfield at δ9.6 ppm as a doublet with coupling constant value of 2.8 Hz. So, with a very simple and efficient protocol we had in hand the helencenic precursor for further extension.

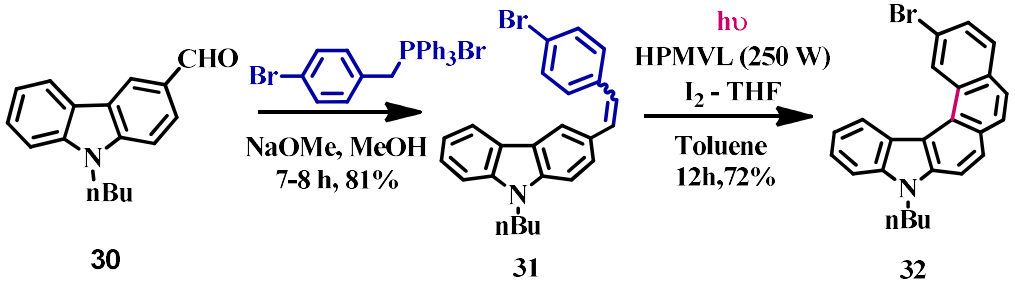

Scheme 3.1.6: Synthesis of bromo-substituted pentahelicene precursor

3.1.2.2 *Synthesis of the heptahelicene from pentahelicene*

The bromo functionality on the precursor opens a window for various chemical transformations; Mizoroki-Heck reaction is one of them which can be utilized for extending the helical scaffold. So helicene **32** was subjected to Heck reaction using a catalyst solution of $Pd(OAc)_2$ and dppp in DMA along with the addition of styrene, K_2CO_3, TBAB and DMA (as solvent) to the reaction flask. The reaction proceeded smoothly at 140°C for 48 hours

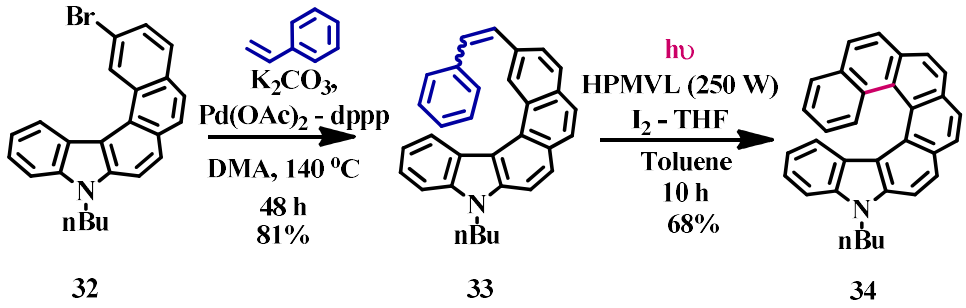

Scheme 3.1.7: Synthesis of heptahelicene from pentahelicene precursor

and resulted in yellow solid of 9-butyl-2-styryl aza[5]helicene **33** with high yield of 81.2% . Olefin **33** was then subjected to standard photocyclization conditions using iodine and tetrahydrofuran (acid scavenger) in toluene as solvent. Careful monitoring (by TLC) of the reaction mixture indicated the formation of a new product within 10 hours. However there are two possibilities as shown in scheme 3.1.8: the cyclization may proceed via the more desirable angular mode yielding 5-butylaza[7]helicene (**34**) or it may proceed via the linear mode yielding the naphthyl substituted aza[5]helicene (**35**). If the product of

cyclization is compound **35**, then the ^{1}H-NMR analysis will clearly show two singlet signals which will be missing if the result is angular cyclization. As shown in figure 3.1.2, in the aromatic region of the ^{1}H-NMR spectrum, no singlet signal can be traced. Moreover, the signals appear relatively upfield after cyclization, which is possible only in angularly cyclized product due to the shielded protons of the overlapping benzene rings.

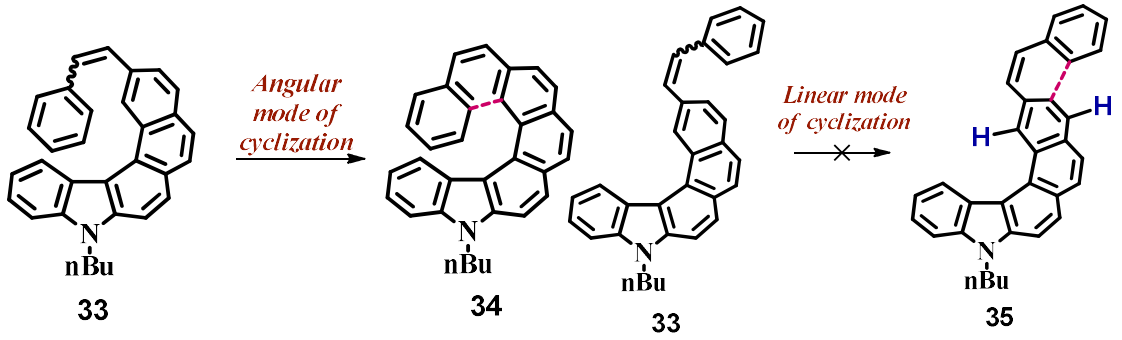

***Scheme 3.1.8**: Modes of the cyclization for the heptahelicene precursor*

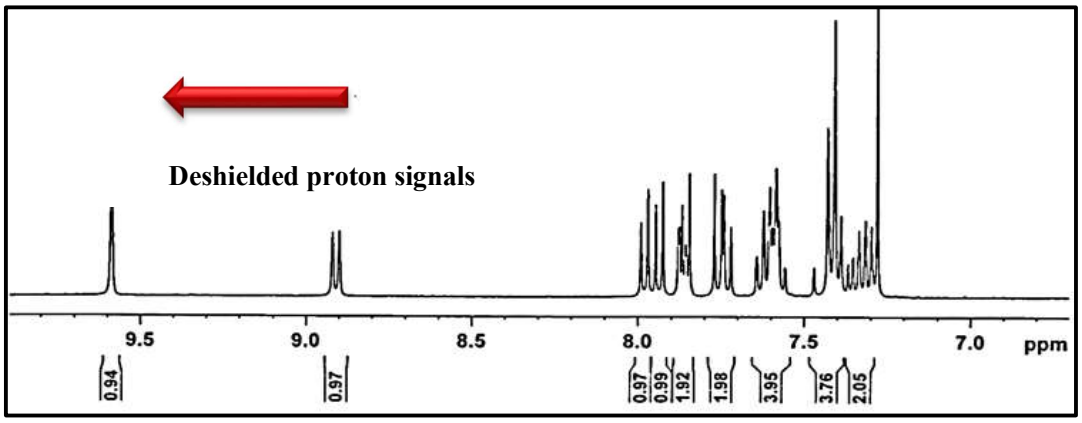

***Figure 3.1.1**: ^{1}H-NMR spectrum of olefin (33)*

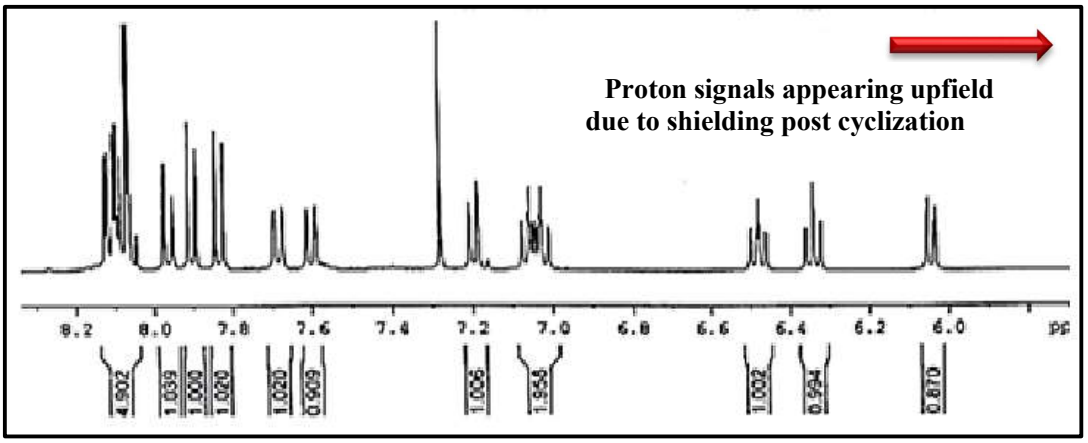

***Figure 3.1.2** : ^{1}H-NMR spectrum of the cyclized product*

3.1.2.3 *Solid state structure analysis of heptahelicene 34*

The heptahelicene was further characterized by single crystal X-ray diffraction analysis. A suitable single crystal was obtained from crystallization in dichloromethane as solvent. The crystal structure indicates a high degree of distortion of the molecular

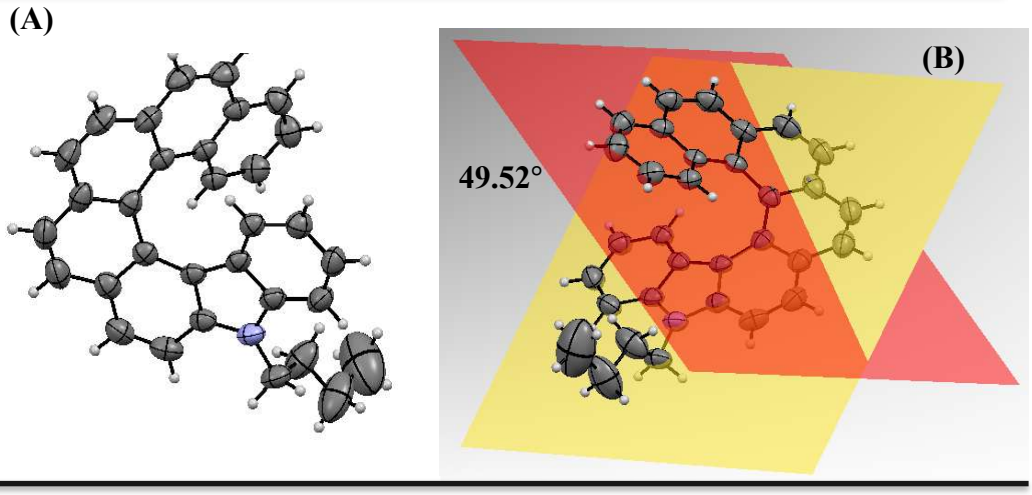

***Figure 3.1.3:** (A) ORTEP plot of compound 34 (CCDC2089757) (B) figure showing dihedral angle of 49.52°*

structure which is the sum of torsion angles. The dihedral angle was found to be 49.52°. The crystal is in orthorhombic lattice with Pbca space group. As typical for a helical geometry, the molecule has characteristic long and short C-C bonds. In the outer helical rim, the average bond length is 1.351 Å contributed by C21-C22 (1.355 Å), C2-C3 (1.342 Å), C5-C6 (1.329 Å), C8-C9 (1.361 Å) and C11-C12 (1.371 Å) which is shortened by 0.042 Å relative to the average bond length in aromatic compounds. Contrary to this, the C-C bond length of the inner helix consisting of C14-C15 (1.417 Å), C15-C16 (1.452 Å), C16-C17 (1.442 Å), C17-C18 (1.450 Å), C18-C19 (1.425 Å), C19-C23 (1.457 Å), and C23-C24 (1.391 Å) with an average bond length of about 1.437 Å showed an increase of 0.044 Å. This change in bond length arising out of intramolecular torsion due to helical geometry is consistent with earlier reports of similar helical system. The torsion angles along the inner helical rim are 4.05º (φ1=C24-C23-C19-C18), 13.28º (φ2=C23-C19-C18-C17), 27.23º (φ3=C19-C18-C17-C16), 27.54º (φ4=C18-C17-C16-C15) and 13.85º (φ5=C17-C16-C15-C14). The crystal structure indicates a high degree of distortion of the

molecular structure which is evident from the sum of three torsion angles (φ1+φ2+φ3=44.56º and φ3+φ4+φ5=68.62º).

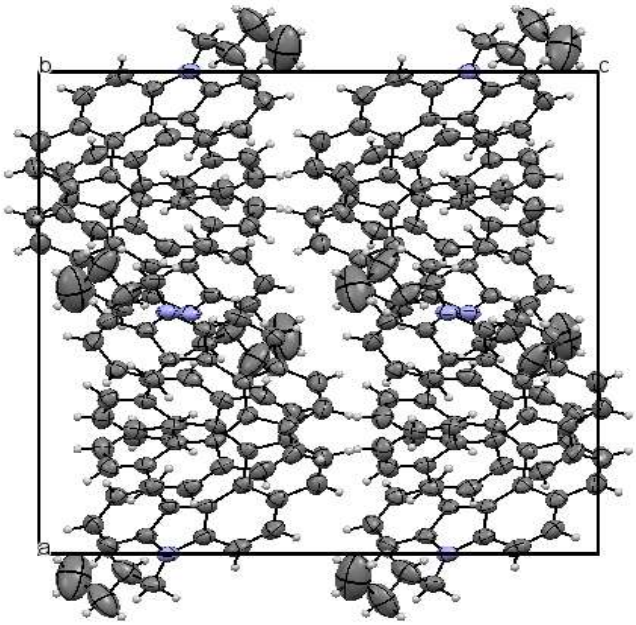

***Figure 3.1.4**: Crystal packing along the 'b' axis*

3.1.2.4: *Thermal Properties*

Thermal properties of compound **34** were investigated by thermogravimetric analysis and differential scanning calorimetry with heating and cooling rates of 10 °C min^{-1} under inert atmosphere. It is essential to have good thermal stability to endure joule heating during prolonged device operation. In the DSC analysis, the first endothermic peak was found at the melting temperature (T_m) of 198.2 °C and the decomposition temperature (T_d) which indicates the temperature at which there is a 5% weight loss was found to be 317 °C indicating high thermal stability. (Figure 3.1.5). The differential scanning calorimetry also showed a high glass transition temperature of 117.8 °C which is a great asset to OLED application.

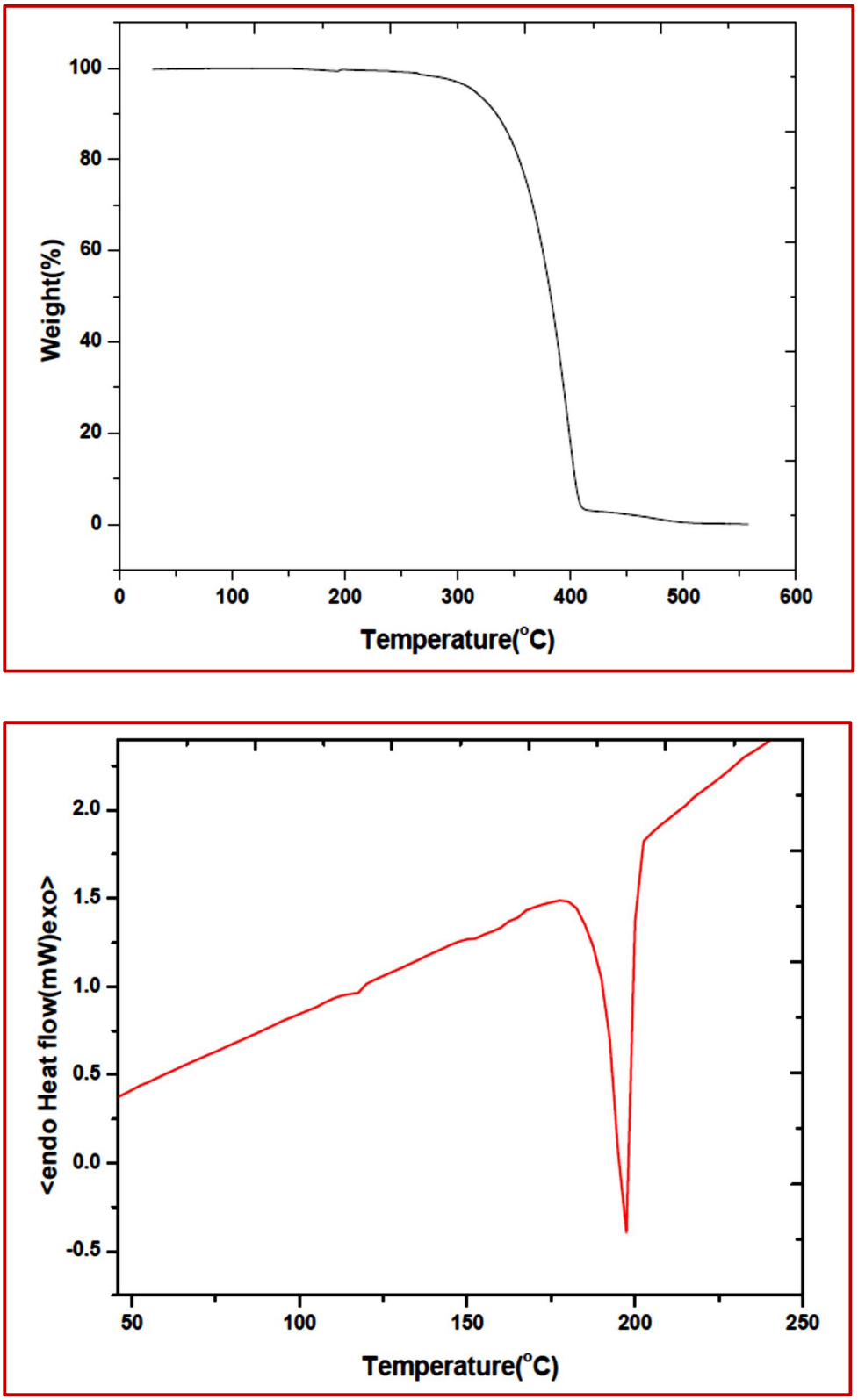

Figure 3.1.5: TGA and DSC curve for compound 34

3.1.2.5: *Electrochemical Properties*

Cyclic voltammetry (CV) was used to understand the electrochemical behaviour of compound **34**. The pyrrolo[7]helicene was dissolved in acetonitrile at 10^{-4} M with 0.1 M NBu_4PF_6 as the supporting electrolyte. A three-electrode cell with Pt electrode, a glassy carbon electrode and a saturated Ag/AgCl electrode was employed as auxiliary, working and reference electrodes respectively. The potential of the reference electrode in acetonitrile was calibrated by using the ferrocene/ferrocenium (Fc/Fc^+) redox system. The cyclic voltammogram in anodic and cathodic scans is shown in figure 3.1.6. The oxidation peak was at 0.972 V with its onset oxidation potential of 0.556 V. The reduction peak was found at -0.827 V. The highest occupied molecular orbital (HOMO) level was calculated using the onset oxidation potential according to the equation HOMO = $-e(E_{onset(ox)} - E_{1/2,FOC}) - 4.8$ eV, which is equivalent to the ionization potential. This was estimated to be -5.239 eV.

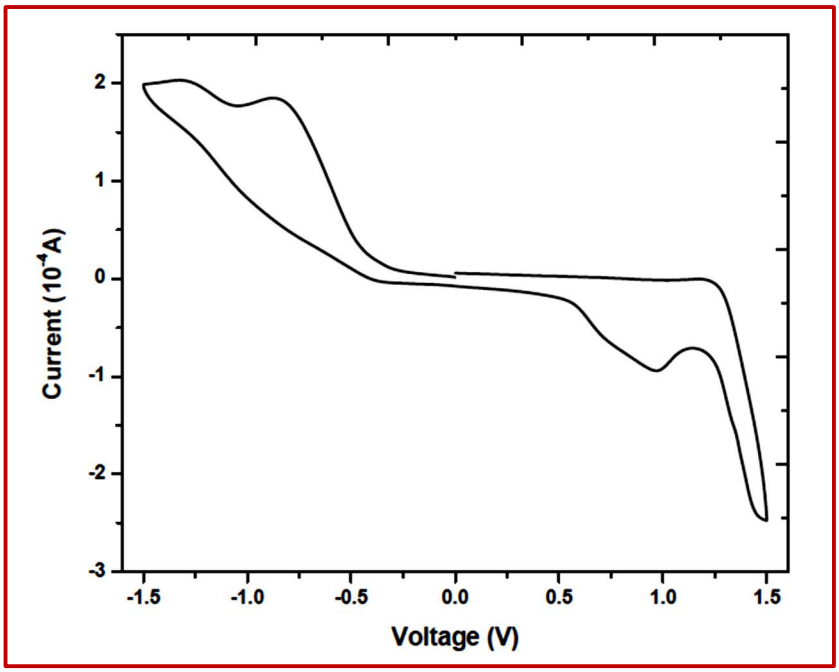

***Figure 3.1.6**: Cyclic voltammogram of 34 in acetoniltrile at a scan rate of 300 mVs^{-1}*

3.1.2.6: *Quantum chemical calculations*

Quantum chemical calculations were carried out for compound **34** using the Gaussian 09 program to perceive the electronic structures. Using the B3LYP function with 6-31G(d,p) basis sets we computed the optimized geometry for the molecule with density functional theory. The optimized geometry and the frontier molecular orbitals are shown in figure 4. The energy of the HOMO and LUMO orbitals were estimated to be -5.0586 eV and -1.2931 eV respectively. Accordingly the the band gap by theoretical calculation was 3.7 eV

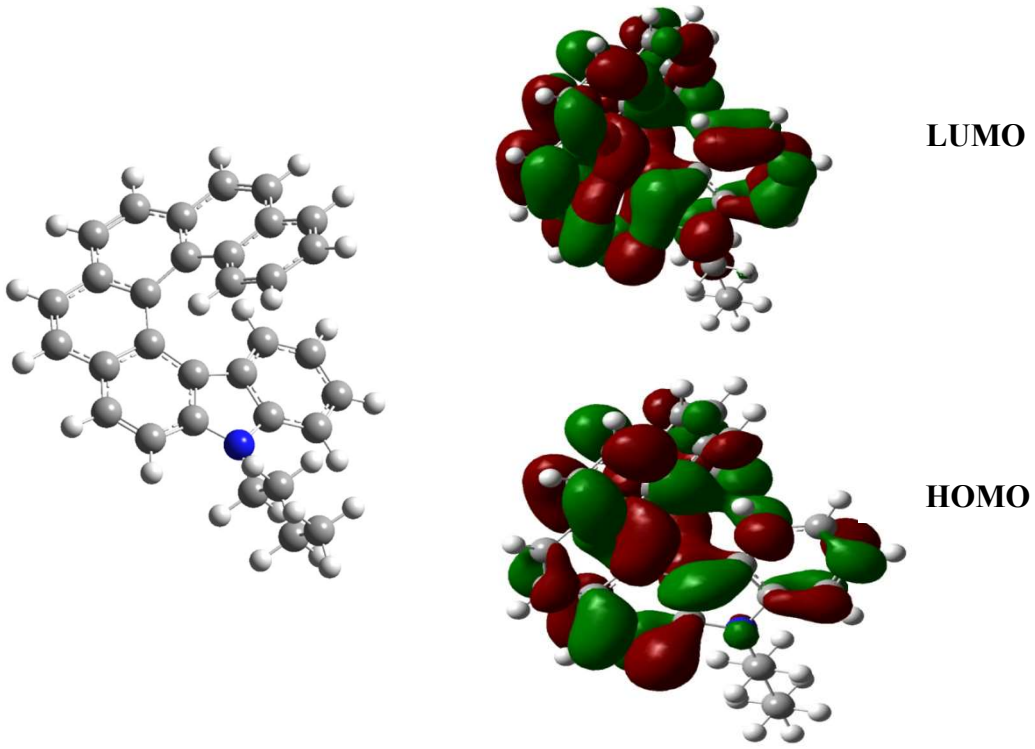

***Figure 3.1.7** : Optimized geometry and HOMO and LUMO orbitals of 34*

3.1.2.7 *Functionalization of the heptahelicene*

Post-synthesis functionalization of helicene via substitution on the helical scaffold opens new arena for the synthesis of chiral functionalized materials. We carried out Vilsmeier-Haack formylation of compound **34** using DMF and $POCl_3$. However, the resultant mono-formylated product was a mixture of two isomers which was separated by column chromatography and analysed by ^{1}H-NMR spectroscopy to confirm the site of

formylation. A significant shift was seen in the aldehydic proton peak in both the isomers. One of the compounds showed the aldehydic proton peak at 9.26 ppm which was relatively upfield compared to 10.55 ppm indicating that the formyl group in one of the isomers was considerably shielded by the terminal aromatic rings owing to ring current effect. Thus, the site of formylation was confirmed to be C-2 and C-9 based on ^{1}H-NMR analysis. Next we carried out several experiments to optimize the reaction condition but in all the cases, the 9-formyl derivative was the major product. Nonetheless both the isomers could be easily separated by column chromatography and crystallization. This was further confirmed from SCXRD analysis as we were able to grow good quality single crystal for both the isomers.

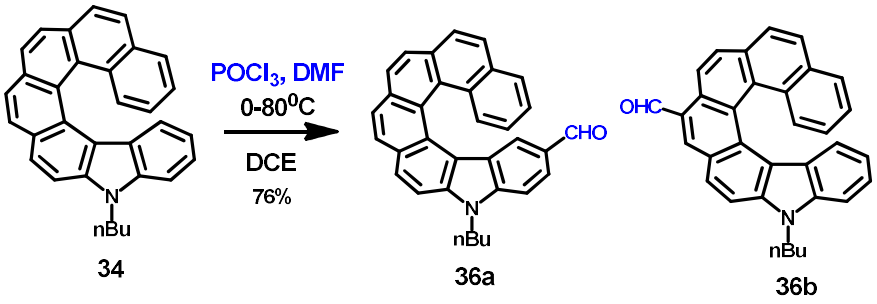

Scheme 3.1.9: Vilsmeier-Haack formylation of compound 34

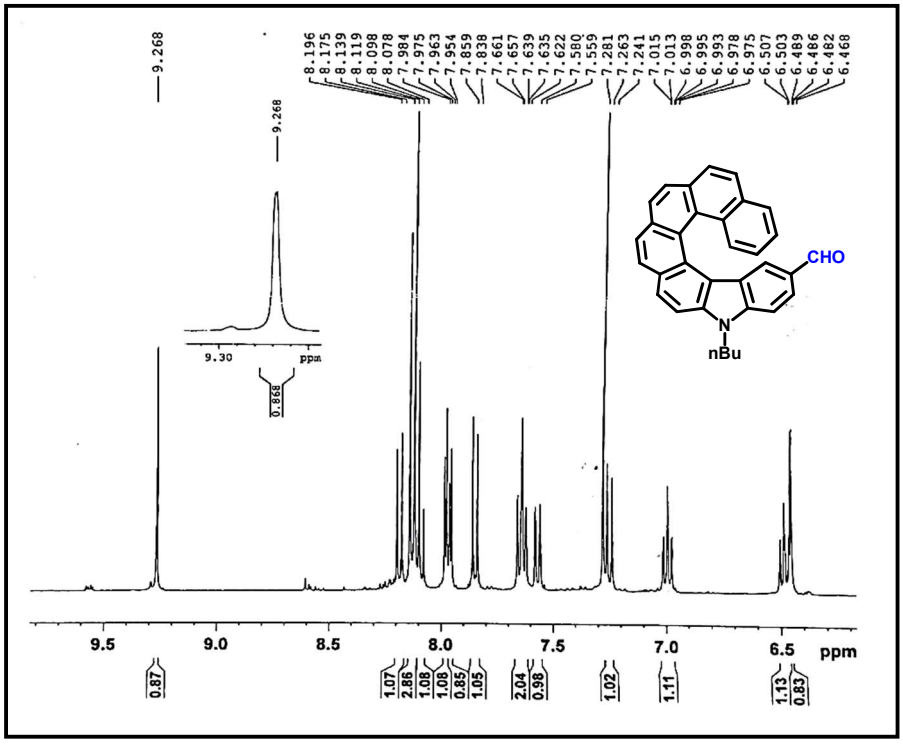

Figure 3.1.8 : Aromatic region of ^{1}H-NMR spectrum of 36a

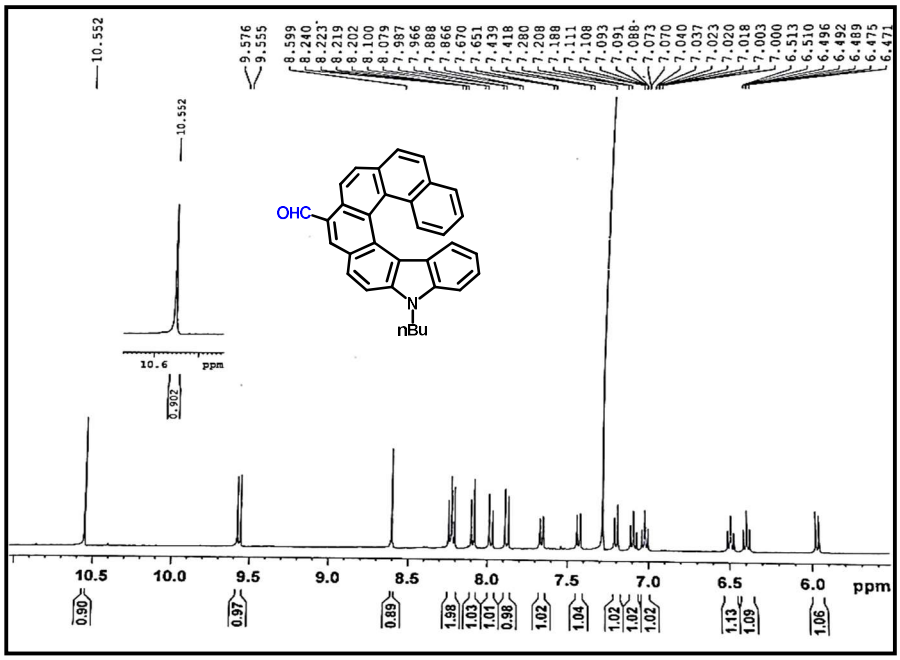

***Figure 3.1.9:** Aromatic region of ^{1}H-NMR spectrum of 36b*

The 2-formyl derivative of the Vilsmeier reaction product was more preferrable for further studies as the functional group was under the influence of the helical scaffold. Thus, we tried to optimize the reaction conditions for the formation of the desired compound **36a**. The experiments showed that in all the conditions that were attempted, the major product was **36b** and under harsh conditions, it was difficult to control the regioselectivity and mixture of products were obtained. With one equivalent each of $POCl_3$ and DMF, there was no formation of product. The thin layer chromatography after 12h showed only a single spot corresponding to the starting material. When the temperature was maintained between 75-80 ℃, the TLC analysis showed the formation of compound **36b** with only trace amount of **36a** when 2 and 5 equivalents of DMF and $POCl_3$ was used. It was observed that on increasing the temperature to 90-95 ℃ under the same condition, yield of 36a was much improved and a 60:40 ratio of **36b** and **36a** was obtained when the ratio of $POCl_3$ and DMF was 5:2. On increasing the equivalents further, the TLC analysis showed a mixture of spots but none corresponding to the mono-formylated products **36a** and **36b**. Under increased molar equivalents, when the temperature was raised beyond 90 ℃, again there was formation of mixture of diformylated products.

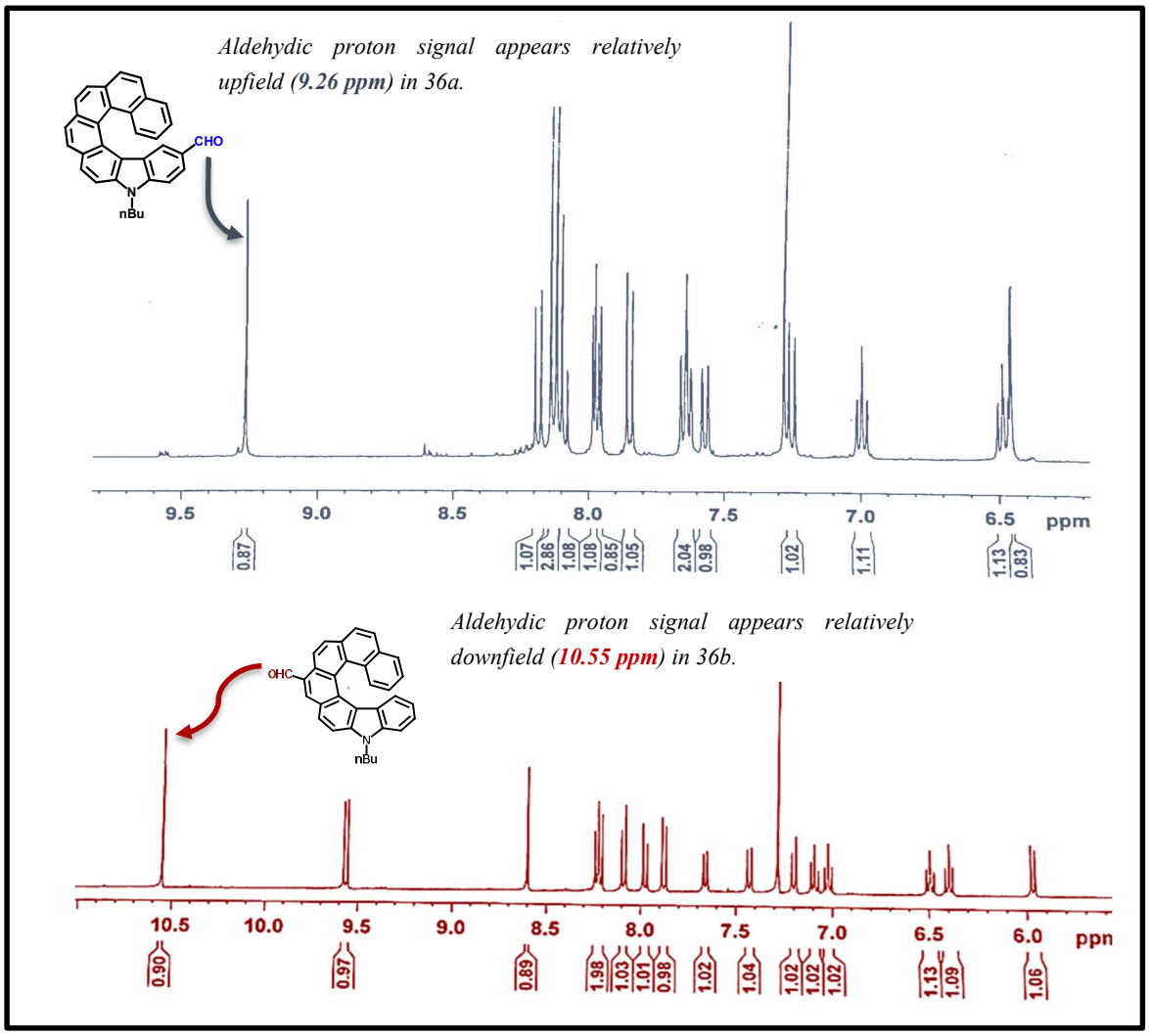

***Figure 3.1.10**: Comparison of ^{1}H NMR signals of 36a and 36b*

3.1.2.8 *Solid state structure analysis of formyl helicenes*

The formyl derivatives of aza[7]helicene were also further characterized by single crystal X-ray diffraction analysis. Compounds 36a and 36b were crystallized by slow evaporation in dichloromethane solvent. The compound 36a crystallized out in $P2_1/n$ space group while 36b crystallized out in *P*ccn space group. The site of substitution on the helical scaffold considerably affects the twist or distortion in the skeleton as is evident from the structural parameters of these compounds. The torsion angles for the compounds along the inner helical rim are 13.47º (φ1=C8-C9-C13-C7), 30.61º (φ2= C9-C13-C7-C5), 24.79º (φ3= C13-C7-C5-C1), 15.21º (φ4= C7-C5-C1-C3) and 3.92º (φ5= C5-C1-C3-C11) for 36a while 11.12º (φ1=C26-C23-C22-C1), 11.05º (φ2=C23- C22-C1-C2), 23.07º (φ3= C22-C1-C2-C3), 31.40º (φ4= C1-C2-C3-C4) and 14.79º (φ5= C2-C3-C4-C5) for 36b. Thus, the sum of three torsion angles is 68.87(φ1+φ2+φ3) and 43.92(φ3+φ4+φ5) for 2-formyl helicene whereas for 9-formyl helicene it is 45.24º(φ1+φ2+φ3) and 69.26º (φ3+φ4+φ5). The dihedral angle was calculated to be 44.78º for 9-formyl helicene and 54.80º for 2-formyl helicene.

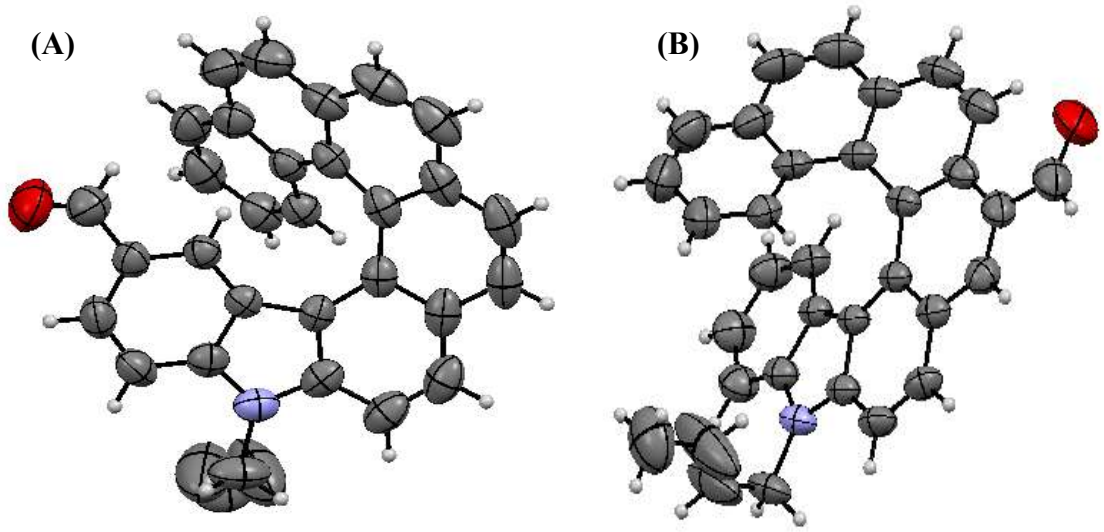

Figure 3.1.11: *(A) ORTEP plot of 36a (CCDC2023651) and (B) ORTEP plot of 36b (CCDC2023652)*

(A)

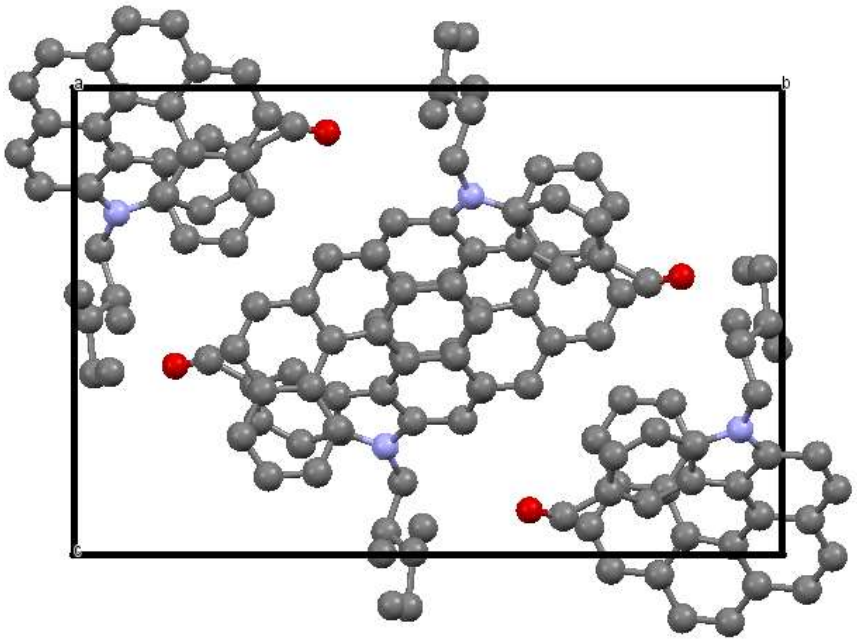

(B)

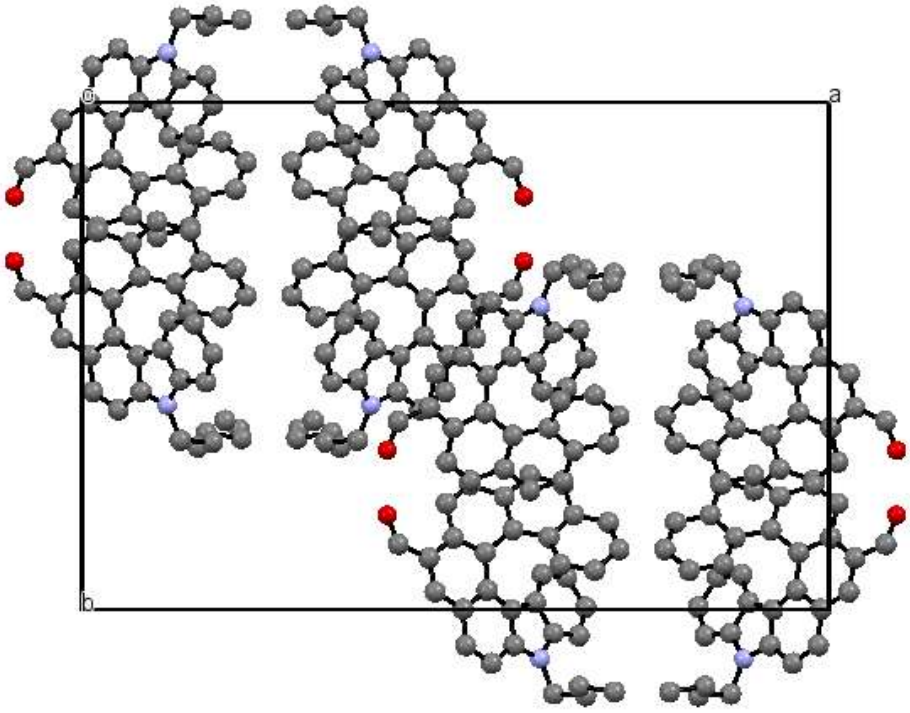

Figure 3.1.12: *(A) and (B) are the corresponding crystal packing structures along the 'c' axis for compounds 36a and 36b respectively*

3.1.2.9 *Synthesis of chiral helical amine*

In order to access chiral functionalized unsymmetrical pyrrolo[7]helicene we carried out resolution utilizing the aldehydic group via diastereomeric separation with (*S*)-phenylethylamine. The compound 36a was subjected to reductive amination in the presence of the chiral amine and titaniumtetraisopropoxide (TTIP) was added to generate the imine which was in-situ reduced using sodiumcyanoborohydride to the corresponding amine. However, the reaction resulted in multiple non-polar spots and the only polar spot which was isolated by purification from column chromatography was the chiral helical amine derivative with (*M*)-configuration. The structure was confirmed by ^{1}H NMR analysis and the absolute configuration of helical structure was tentatively assigned to be *M* based on the optical rotation value, which was in minus sign (-5352 in dichloromethane). It is a unique property of helicenes to exhibit very high specific optical rotation values and the value obtained for the levorotatory helicene **37** is in the range of the optical rotation values for other seven-membered helical molecules.

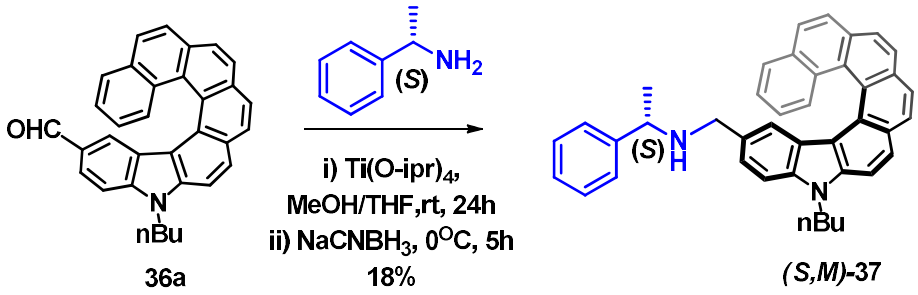

***Scheme 3.1.10**: Synthesis of chiral helical amine ligand*

3.1.2.10 *Photophysical properties*

The aza[7]helicene, the formyl derivative and the amine were investigated using UV-Vis absorption and fluorescence emission study performed in chloroform solution (5.0×10^{-5} mol). A strong absorption was exhibited in the region of 253-325 nm. Absorption maxima for the helicene appears at 253 nm while that for the formyl derivative it is around 254 nm, followed by peaks of medium intensity at 325-350 nm. These absorption bands in the region between 250 and 350 nm correspond with the π–π* and n-π* electronic tranistions. The heptahelicene exhibited a deep blue emission peak at 440 nm and a shoulder peak at 465 nm. The emission of the formyl derivative was found to be at 467 nm. The fluorescence quantum yield of compound **34** was measured to be 0.192 using quinine sulphate solution (0.5M in H_2SO_4) and excitation of 360 nm. By Tauc's plot, the Eg for compound 34 was calculated to be 3.25 eV.

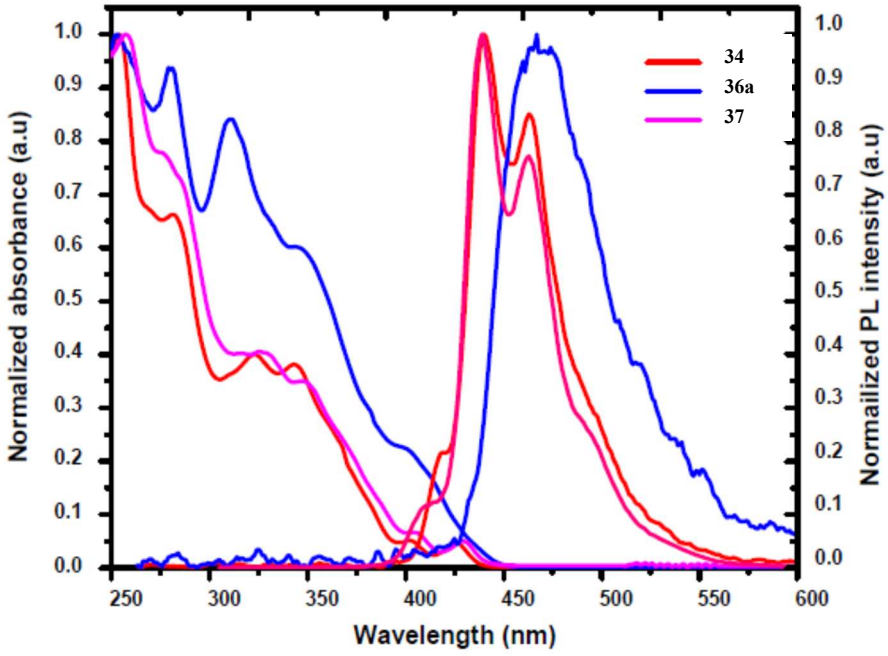

34	254	440	186
36a	253	467	214
37	256	442	186

3.1.3 Conclusion

In conclusion, we have developed a facile method for the synthesis of carbazole based pyrrolo[7]helicene with an unsymmetrical scaffold. The thermal, electrochemical, optical, and structural parameters of this helicene were completely investigated. Electrophilic substitution reaction on this unsymmetrical framework, rendered two isomers which were characterized by single crystal XRD analysis. This functionalized core then provided means for the synthesis of chiral amine ligand of pyrrolo[7]helicene by in-situ reductive amination reaction.

3.1.4 Experimental Data

Synthetic procedures and analytical data

9-butyl-9*H*-3-(4-bromostyryl)-9H-carbazole (31)

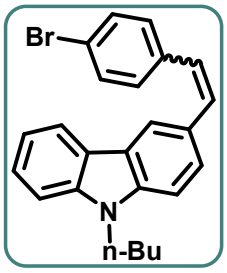

Molecular formula: $C_{24}H_{22}BrN$
Molecular weight: 404.34
Physical state: white crystalline solid
$\mathbf{R_f}$=0.4 (1:99 EtOAc/petroleum ether).
M.p = 195-197 ^{0}C.

In a two-necked round bottom flask stoppered on one end and septa placed on the other end, which was degassed and purged with nitrogen, a solution of 9-butyl-3-formyl carbazole (2.0g, 7.96 moles) and 4-bromobenzyltriphenylphosphonium bromide (4.9g, 9.55 mmol) in dry methanol (20 mL) was added and kept for room temperature stirring. To this mixture, a solution of sodium metal (0.275g, 11.94 mmol) dissolved in dry methanol (10 mL) was added dropwise and the reaction mixture was stirred vigorously for 7-8 hours. After the completion of reaction (monitored by TLC), ethanol was evaporated under reduced pressure, the reaction mixture was poured on ice cold water (50mL) and extracted using ethyl acetate (3 x 50 mL). Combined organic layer was washed with water (50mL) and dried over anhydrous sodium sulfate and concentrated at reduced pressure. Compound was purified by performing column chromatography over silica gel using Pet Ether: Ethyl acetate (98:2) as eluent. Yield**:** 2.62g (81.37%)

^{1}H NMR (400 MHz, $CDCl_3$) : δ 8.24 (d, *J*=1.2Hz, 1H), 8.14 (d, *J*=7.6Hz, 1H), 7.68 (d, *J*=10Hz, 1H), 7.51-7.47 (m, 3H), 7.44-7.40 (m, 4H), 7.32 (d, *J*=16.4, 1H), 7.29-7.25 (m, 4H), 7.09 (d, *J*=16.4, 1H), 4.33 (t, *J*=14.4, 2H), 1.89 (m, 2H), 1.47-1.38 (m, 2H), 0.97 (t, *J*=14.4, 3H)

9-butyl-9*H*-2-bromoaza[5]helicene (32)

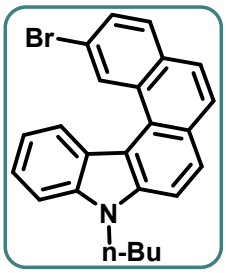

Molecular formula: $C_{24}H_{20}BrN$
Molecular weight: 402.33
Physical state: white crystalline solid
R_f =0.4 (1:99 EtOAc/petroleum ether).
M.p = 178-180 ^{0}C.

A solution of 9-butyl-3-(4-bromostyryl)-9H-carbazole (0.8g, 2 mmol), iodine (0.553g, 2.2 mmol), THF (7.2g, 8.05mL, 100 mmol) and Toluene (1.2 litres) was taken in an immersion wall photo reactor (borosilicate glass) equipped with water cooling jacket and a stir bar. It was irradiated using a 250W HPMV lamp for 12-13hrs monitored by TLC. After the completion of reaction, excess of iodine was removed from the mixture by treating it with a solution of sodium thiosulfate, followed by distilled water. The organic layer was concentrated under reduced pressure which gave crude product. Purification of crude product was done by performing column chromatography over silica gel using Pet Ether: Ethyl acetate (98:2) as eluent. **Yield:** 0.556g (71.11%)

^{1}H NMR (400 MHz, $CDCl_3$): δ 9.66 (s, 1H), 8.85 (d, *J*=7.6Hz, 1H), 7.90-7.84 (m, 3H), 7.77-7.68 (m, 3H), 7.60 (s, 2H), 7.40 (d, *J*=5.6Hz, 1H), 4.45 (s, 2H), 1.94 (t, *J*=14Hz, 2H), 1.52-1.33 (m, 2H), 1.01 (t, *J*=14.4, 3H)

^{13}C NMR (100 MHz, $CDCl_3$): 140.2, 131.5, 130.8, 130.2, 129.4, 129.2, 127.9, 127.3, 127, 126.8, 125.2, 123.3, 123.1, 118.7, 118.2, 116.4, 110.7, 109.3, 43, 31.3, 20.6, 13.9

IR (KBr): 3436, 3046, 2953, 1583, 1464, 1329, 1151, 835, 742 cm^{-1}

9-butyl-9*H*-2-styryl aza[5]helicene (33)

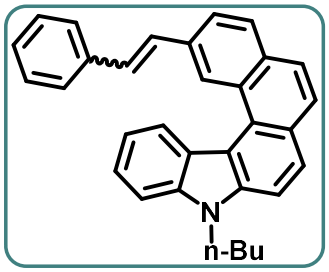

Molecular formula: $C_{32}H_{27}N$
Molecular weight: 425.56
Physical state: white crystalline solid
R_f =0.4 (2:98 EtOAc/petroleum ether).
M.p = 185-187 ^{0}C.

A catalyst solution was prepared under nitrogen atmosphere using $Pd(OAc)_2$, (0.0034g, 0.013 mmol, 2 mol%) and dppp (0.0123g, 0.026 mmol, 4 mol%) in DMA (5mL) at room temperature with constant stirring until a homogenous solution was obtained. A two-necked round bottom flask was charged with 9-butyl-2-bromoaza[5]helicene (0.3g, 0.746 mmol), styrene (0.094g, 0.104 mL, 0.904 mmol), dry K_2CO_3 (0.42g, 3 mmol), TBAB (0.484g, 1.5 mmol, 20 mol%) and DMA (15mL), and the mixture was heated up to 100°C. At 100°C, the catalyst solution was added dropwise, and the mixture was heated to 140°C for 48 hours. After the completion of the reaction, the mixture was poured into water and extracted with ethyl acetate (3 x 100 mL). The combined organic phase was washed with water, brine and dried over anhydrous sodium sulfate. The solvent was removed under reduced pressure and the crude product was purified by column chromatography on silica gel using Pet ether: Ethyl acetate (95:5) as eluent to afford cis-trans isomers of 9-butyl-2-styryl aza[5]helicene. **Yield:** 0.244g (81.2%)

^{1}H NMR (400 MHz, $CDCl_3$) : δ 9.59 (s, 1H), 8.91 (d, *J*=8Hz, 1H), 7.98 (d, *J*=8Hz, 1H), 7.94 (d, *J*=8.4, 1H), 7.88-7.85 (m, 2H), 7.77-7.72 (m, 2H), 7.64-7.56 (m, 4H), 7.47-7.39 (m, 4H), 7.37-7.28 (m, 2H), 4.53 (t, *J*=14.4, 2H), 2.0-1.97 (m, 2H), 1.55-1.49 (m, 2H), 1.02 (t, *J*=14.8, 3H)

^{13}C NMR (100MHz, $CDCl_3$) : δ 140.28, 140.21, 137.63, 133.69, 132.65, 129.79, 129.06, 128.73, 128.46, 128.18, 128.01, 127.64, 127.55, 127.41, 127.14, 126.61, 126.35, 125.06, 124.80, 123.74, 123.63, 123.36, 118.39, 116.66, 110.21, 109.33, 77.37, 77.25, 77.05, 76.73, 43.03, 31.38, 20.63, 13.94

IR (KBr) : 3446.8, 3048, 3024, 2954, 1588, 1469, 1331, 1151, 962.5, 827.6, 747 cm^{-1}

HRMS(ESI-TOF): m/z calcd. for $[C_{32}H_{27}N+Na]^+$ is 448.2030; found, 448.2035.

5-butyl-5*H*-aza[7]helicene (34)

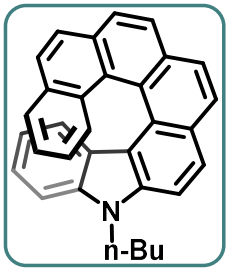

Molecular formula: $C_{32}H_{25}N$
Molecular weight: 423.55
Physical state: white crystalline solid
R_f =0.4 (2:98 EtOAc/petroleum ether).
M.p = 198 ^{0}C.

A solution of 9-butyl-2-styrylaza [5] helicene (0.3g, 0.71 mmol), iodine (0.232g, 0.91 mmol), dry THF (2.993g, 3.4mL, 41.5 mmol) and toluene (600 mL) was irradiated using a 125W HPMV lamp (8 h monitored by TLC). After the completion of reaction, excess of iodine was removed from the mixture by treating it with a solution of sodium thiosulfate, followed by distilled water. The organic layer was concentrated under reduced pressure which gave crude product. Purification of crude product was done by performing column chromatography over silica gel using Pet ether: Ethyl acetate (95:5) as eluent to obtain 5-butyl- aza[7]helicene. **Yield:** 0.135g (67.83%)

^{1}H NMR (400 MHz, $CDCl_3$) : δ 8.12-8.07 (m, 5H), 7.96 (d, J=8.8, 1H), 7.90 (d, J=8Hz, 1H), 7.83 (d, J=8.8, 1H), 7.68 (d, J=8.8, 1H), 7.60 (d, J=8.8, 1H), 7.19 (d, J=8Hz, 1H), 7.07-7.01 (m, 2H), 6.50-6.48 (m, 1H), 6.36-6.32 (m, 1H), 6.04 (d, J=8Hz, 1H), 4.43 (t, J=14.4Hz, 2H), 1.89 (t, J=15.2Hz, 2H), 1.43 (t, J=15.6, 2Hz), 0.99 (t, J=14.8, 3H)

^{13}C NMR (100MHz, $CDCl_3$) : δ 138.8, 138.5, 133.1, 132.2, 130.4, 128.5, 127.8, 127.4, 127.2, 126.6, 126.4, 126.3, 125.7, 125.6, 123.7, 123.6, 123.5, 123.1, 121.8, 117.9, 117.2, 110.6, 107.6, 42.7, 31.2, 20.4, 14.0

IR (KBr): ν 3443.4, 3042, 2955.8, 1608.4, 1580.5, 1465.8, 1331.7, 1150, 838.4, 745.4, 607.2 cm^{-1}

HRMS ESI-TOF): m/z calcd. for $[C_{32}H_{25}N]^+$ is 424.2021; found, 424.1953

2-formyl-5-butyl-5*H*-aza[7]helicene (36a)

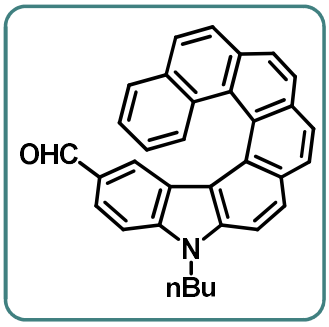

Molecular formula: $C_{32}H_{25}NO$
Molecular weight: 451.19
Physical state: yellow crystalline solid
R_f =0.3 (10:90 EtOAc/petroleum ether).
M.p = >210 ^{0}C.

In a two-necked round bottom flask purged with nitrogen at 0 ℃, phosphoryl chloride (0.29g, 1.89 mmol) was added slowly to DMF (0.34g, 0.36ml, 4.73mmol). This complex was warmed to room temperature after the addition of phosphoryl chloride for 1 hour and then cooled again to 0 ℃. To this complex, the solution of pyrrolo[7]helicene (0.4g, 0.945mmol) in 1,2-dichloroethane (15 mL) was added and then stirred for 8 hours at 90 ℃. The resulting crude mixture was poured into ice water and dried over anhydrous sodium sulphate and concentrated at reduced pressure. The purification of the compound was carried out by column chromatography over silica gel using 10% ethyl acetate-petroleum ether to render the formyl derivative as yellow solid.

^{1}H NMR (400 MHz, $CDCl_3$): δ 9.27 (s, 1H), 8.18 (d, *J*=8.4 Hz, 1H), 8.12 (d, *J*=8 Hz, 3H), 8.08 (d, *J*=8 Hz, 1H), 7.97 (d, *J*=8.4 Hz, 1H), 7.96 (d, *J*=8.4 Hz, 1H), 7.84 (d, *J*=8.4 Hz, 1H), 7.64 (dd, J_1=8.8 Hz, J_2=1.6 Hz, 1H), 7.63 (d, *J*=6.8 Hz, 1H), 7.57 (d, *J*=8.4 Hz, 1H), 7.25 (d, *J*=8.8 Hz, 1H), 6.99 (m, 1H), 6.49 (m, 1H), 6.45 (d, *J*=1.6 Hz, 1H), 4.45 (t, *J*=7.2 Hz, 2H), 1.92 (m, 2H), 1.42 (m, 2H), 1.00 (t, *J*=7.2 Hz, 3H);

9-formyl-5-butyl-5*H*-aza[7]helicene (36b)

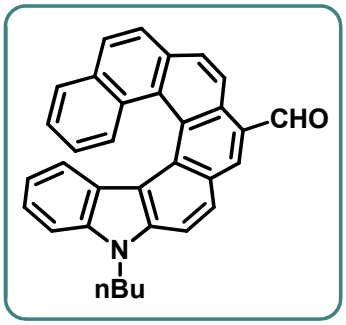

Molecular formula: $C_{32}H_{25}NO$
Molecular weight: 451.19
Physical state: yellow crystalline solid
R_f =0.3 (10:90 EtOAc/petroleum ether).
M.p = >210 ^{0}C.

: **^{1}H NMR (400 MHz, $CDCl_3$):** d 10.55 (s, 1H), 9.56 (d, *J*=8.4 Hz, 1H), 8.59 (s, 1H), 8.22 (d, *J*=8.4 Hz, 1H), 8.21 (d, *J*=8.4 Hz, 1H), 8.09 (d, *J*=8.4 Hz, 1H), 7.97 (d, *J*=8.4 Hz, 1H), 7.87 (d, *J*=8.8 Hz, 1H), 7.66 (d, *J*=7.6 Hz, 1H), 7.42 (d, *J*=8.4 Hz, 1H), 7.19 (d, *J*=8 Hz, 1H), 7.09 (m, 1H), 7.02 (m, 1H), 6.50 (m, 1H), 6.40 (m, 1H), 5.96 (d, *J*=8 Hz, 1H), 4.43 (t, *J*=7.2 Hz, 2H), 1.89 (m, 2H), 1.42 (m, 2H), 1.00 (t, *J*=7.2 Hz, 3H) ppm;

^{13}C NMR (100 MHz, $CDCl_3$): δ = 193.3, 141.2, 128.9, 127.9, 127.5, 127.4, 126.1, 125.8, 125.7, 124.6, 123.8, 122.7, 121.7, 118.2, 111.3, 108.01, 42.8, 31.2, 20.4, 13.9 ppm

IR (KBr): $\tilde{\nu}$= 3445, 3045, 2951, 2867, 2378, 2309, 1672, 1603, 1574, 1518, 1486, 1464, 1422, 1394, 1360, 1335, 1282, 1242, 1213, 1151, 1103, 1068, 889, 836, 795, 773, 737, 693, 630, 604, 550 cm^{-1}

EI-MS^{+}: *m/z*: calculated 452.1936 found 452.1739 $[M+H]^{+}$ $[C_{33}H_{25}NO+H]^{+}$

Compound 37

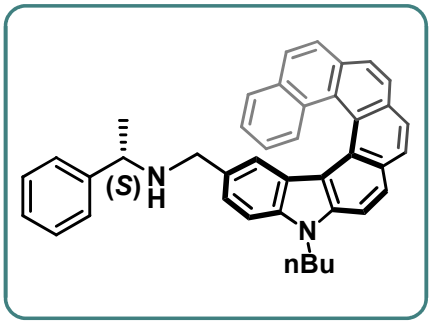

Molecular formula: $C_{41}H_{36}N_2$
Molecular weight: 556.73
Physical state: yellow crystalline solid
R_f =0.3 (40:60 EtOAc/petroleum ether).
M.p = >210 ^{0}C.

To a solution of compound 33a (0.06 g, 0.14 mmol) in anhydrous MeOH/THF (10 mL) was added (*S*)-phenylethylamine (0.02 g, 0.17 mmol), titanium(IV) isopropoxide (0.05 g, 0.17 mmol). The solution was stirred for 24 h at room temperature. Sodium cyanoborohydride (0.01 g, 0.17 mmol) was added to the solution at 0 °C and stirred for 5h. The resulting solution was then poured into 2.0 M aqueous ammonia (10 mL) and the suspension was filtered through Celite and washed with water. The filtrate was extracted with dichloromethane and dried over anhydrous sodium sulphate. Purification of the compound was carried out by column chromatography over alumina using 30% ethyl acetate-petroleum ether as an eluent to render yellow solid. Yield= 18% (0.014 g)

^{1}H NMR (400 MHz, $CDCl_3$): δ= 8.11 (dd, J_1=8 Hz , J_2=2.4 Hz, 2H), 8.08 (s, 2H), 8.03 (d, *J*= 8.8 Hz, 1H), 7.91 (d, *J*=8 Hz, 1H), 7.86 (d, *J*=8.8 Hz, 1H), 7.83 (d, *J*= 8.4 Hz, 1H), 7.56 (m, 2H), 7.37 (m, 2H), 7.32 (m, 3H), 7.14 (d, *J*= 8 Hz, 1H), 7.01 (m, 2H), 6.46 (m, 1H), 5.79 (d, *J*= 0.8 Hz, 1H), 4.42 (t, *J*= 7.2 Hz, 2H), 3.67 (m, 1H), 3.17 (m, 2H), 2.07 (s, 1H), 1.88 (m, 2H), 1.41 (m, 2H), 1.35 (d, *J*=6.4, 3H), 1.27 (m, 3H), 0.98 (t, J= 7.6 Hz, 3H) ppm

^{13}C NMR (100 MHz, $CDCl_3$): δ = 14.2, 20.4, 24.4, 31.3, 42.8, 51.9, 57.4, 107.6, 110.7,117.5, 121.5, 123.0, 123.4, 123.8, 124.7, 125.7, 125.9, 126.3, 126.5, 126.6, 126.8, 126.9, 127.2, 127.5, 128.4, 128.6, 130.4, 130.6, 131.8, 133.2, 137.7, 138.9 ppm

IR (KBr): $\tilde{\nu}$= 3429, 3044, 2955, 2924, 2853, 1679, 1610, 1524, 1454, 1337, 1281, 1243, 1208, 1154, 1107, 1073, 839, 797, 746, 699, 611, 540, 464 cm^{-1}

Mass spectra: *m/z* calculated 556.28 found 556.42 $[C_{41}H_{36}N_2]^+$

3.1.5 Crystallographic Data

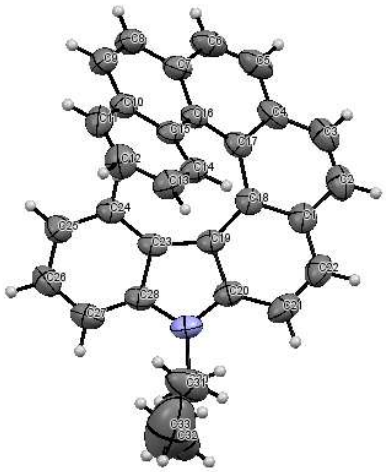

***Figure 3.1.11**: ORTEP plot of compound 34(CCDC 2089757)*

Table 3.1.1: *Crystallographic data of 34*

Identifcation code	CCDC 2089757
Empirical formula	C_{32} H_{25} N
Formula weight	423.53
Crystal System	Orthorhombic
Z, space group	8, Pbca
a (Å)	17.9729 (10)
b (Å)	14.0161 (8)
c (Å)	18.244 (11)
α/^{0}	90
β/^{0}	90
γ/^{0}	90
Volume/Å^3	4595.9
ρcalc g/cm^3	1.224
μ/mm^{-1}	0.070
F(000)	1792
Radiation	MoKα (λ = 0.71073)
Goodness of fit	1.029

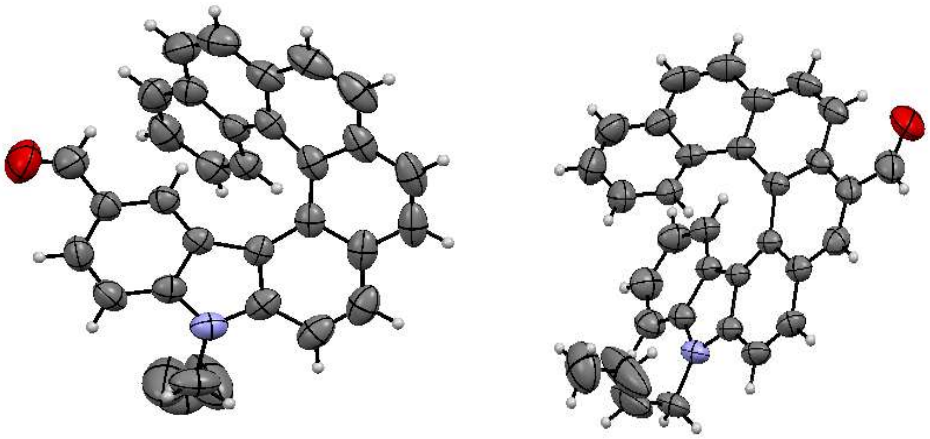

Figure 3.1.12: *ORTEP plot of 36a (CCDC 2023651) and 36b (CCDC2023652)*

Table 3.1.3: ***Crystallographic data of compound 36a and 36b***

Identification code	CCDC 2023651 (36a)	CCDC 2023652 (36b)
Empirical formula	C_{33} H_{25} NO	C_{33} H_{25} NO
Formula weight	451.54	451.54
Crystal System	Monoclinic	Orthorhombic
Z, space group	4, P21/n	8, Pccn
a (Å)	8.9137(9)	29.104(4)
b (Å)	19.9781(18)	19.8035(19)
c (Å)	13.4016(17)	8.2946(11)
α/^{0}	90	90
β/^{0}	100.751(11)	90
γ/^{0}	90	90
Volume/Å^3	2344.7(4)	4780.7(10)
ρcalc g/cm^3	1.279	1.255
μ/mm^{-1}	0.076	0.075
F(000)	952	1904
Radiation	MoKα (λ = 0.71073)	MoKα (λ = 0.71073)
Goodness of fit	1.033	1.011

3.1.6 Computational Analysis

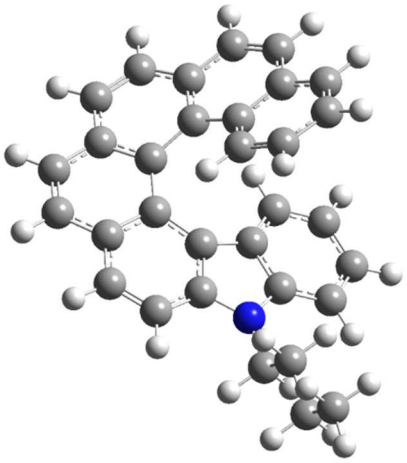

Table 3.1.4: Cartesian coordinates of compound 34

Atomic no.	X	Y	Z
6	-0.000000099	0.000002908	-0.000004567
6	0.000000007	-0.000002195	0.000003495
1	-0.000000937	-0.000000386	0.000000448
6	-0.000000469	-0.000004981	-0.0000032
6	0.000000965	0.000003871	0.000000834
6	-0.000001091	0.000003451	-0.000002901
7	-0.0000002	0.000001124	-0.000007221
6	0.000000171	-0.00000585	0.000000542
6	-0.00000156	-0.000003145	0.000004592
6	0.000001903	-0.000000881	0.000005628
1	0.000000597	-0.000001493	-0.000001037
6	-0.000000908	0.000000305	0.000004219
6	0.000000468	0.00000219	-0.000003097
1	0.000002337	-0.000001063	0.000000813
6	0.00000151	0.000001802	0.000003517
6	0.000001545	-0.000003169	-0.000002315
6	-0.000002791	-0.000001884	-0.000000668
1	0.000001093	0.000001276	0.000001118
6	0.000001219	0.000005643	0.000001878
6	0.000003105	0.000000868	0.000000692
1	0.000000612	-0.000001361	-0.000000917

6	0.000000019	-0.000003789	-0.000003611
6	0.00000049	0.000000487	0.00000456
1	0.000001353	-0.000001681	0.000000122
6	0.000000375	-0.000002679	-0.000000234
1	-0.000001315	0.000000686	-0.000000299
6	0.000000497	0.000001194	-0.000000398
1	0.000001853	-0.00000332	0.00000139
6	0.000000552	-0.000003269	-0.000002942
1	0.000001166	-0.000000314	0.000000545
6	-0.000006347	-0.000000812	-0.000000456
1	-0.000000525	0.000000176	-0.000000696
6	0.00000012	-0.000002646	0.000003195
1	-0.000000295	0.000000142	0.000000649
6	-0.000001337	-0.00000063	-0.000003183
6	0.000002546	0.000001059	0.000004276
1	-0.000000798	0.000000002	-0.000001366
6	0.000003191	0.000002778	-0.000001017
1	0.000000907	0.000000123	0.000000104
6	-0.000001209	-0.000003039	0.000000286
1	-0.000001676	0.000001295	0.000000186
6	0.000000227	0.00000322	0.000001851
1	0.000000648	-0.000002275	0.000000932
6	-0.000001867	-0.000001661	-0.00000191
1	0.000000886	-0.000001147	0.000001558
6	0.000000553	-0.000003039	0.000003255
1	0.000003011	0.000001382	-0.000001038
1	-0.000004221	0.000004197	-0.000003438
6	0.000009521	0.000013241	-0.000004163
1	0.000000051	-0.000005341	-0.000000733
1	-0.000003133	-0.000000817	0.000004448
6	-0.000000056	-0.000010424	-0.000005215
1	-0.000006509	0.000003057	0.000005088
1	-0.000003305	0.00000611	-0.000003596
6	-0.000002546	0.000012597	0.000006767
1	0.000003015	-0.000003566	0.000005261
1	-0.000007913	-0.000001846	-0.000003204
1	0.000004593	0.000003517	-0.000008826

3.1.7 Spectral Data

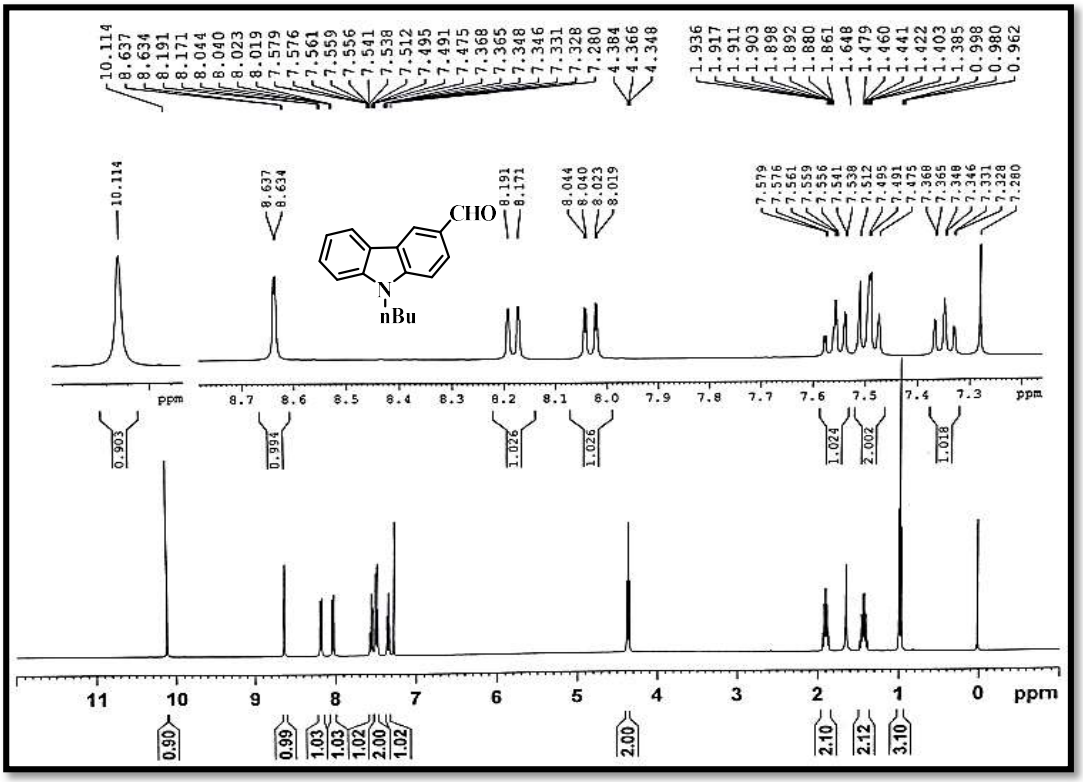

^{1}H NMR spectra of 9-butyl-3-formyl-9*H*-carbazole

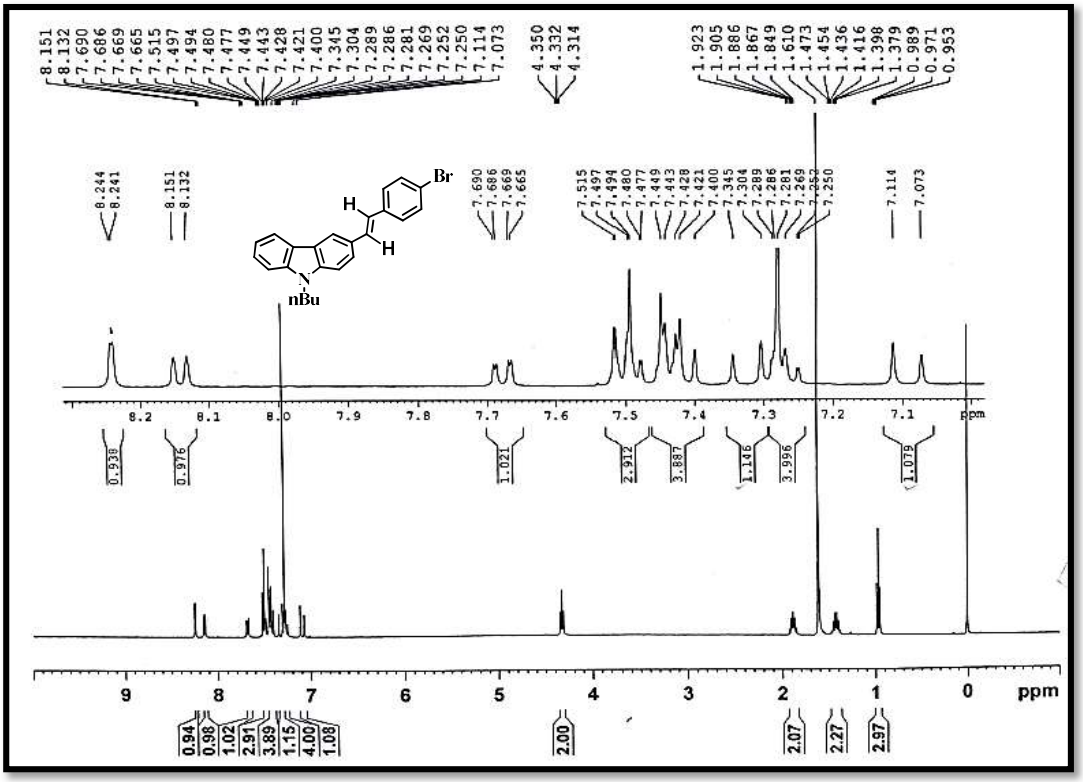

^{1}H NMR spectra of compound 31

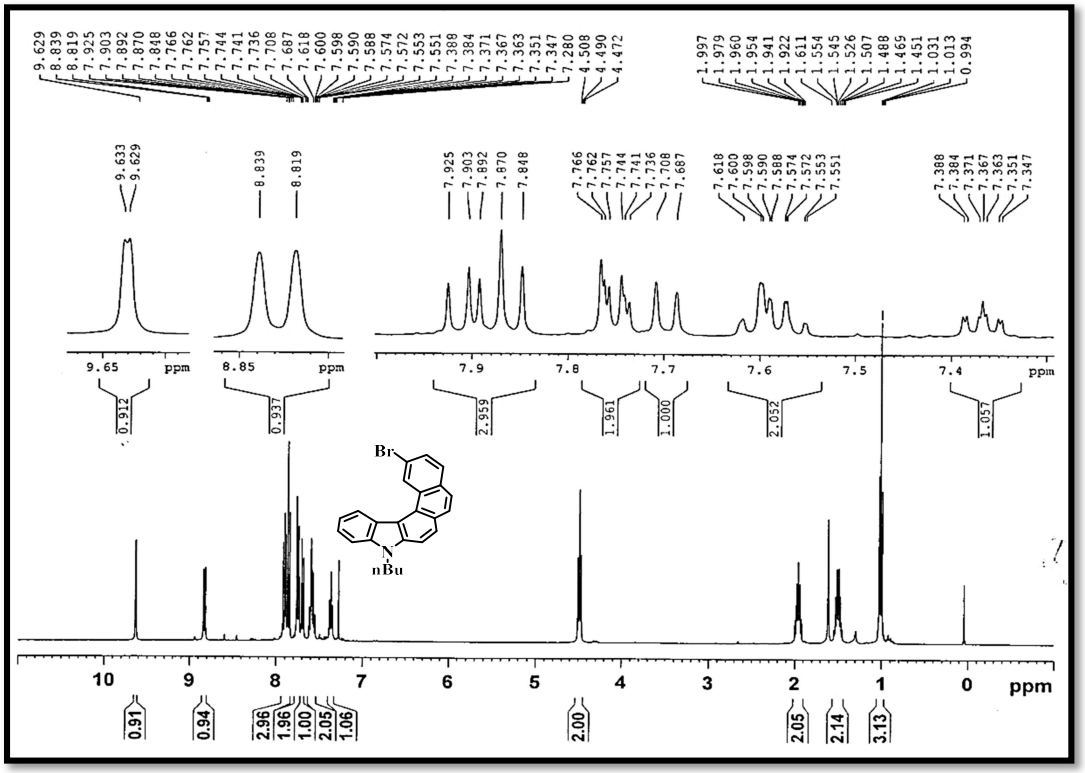

[1]H NMR spectra of compound 32

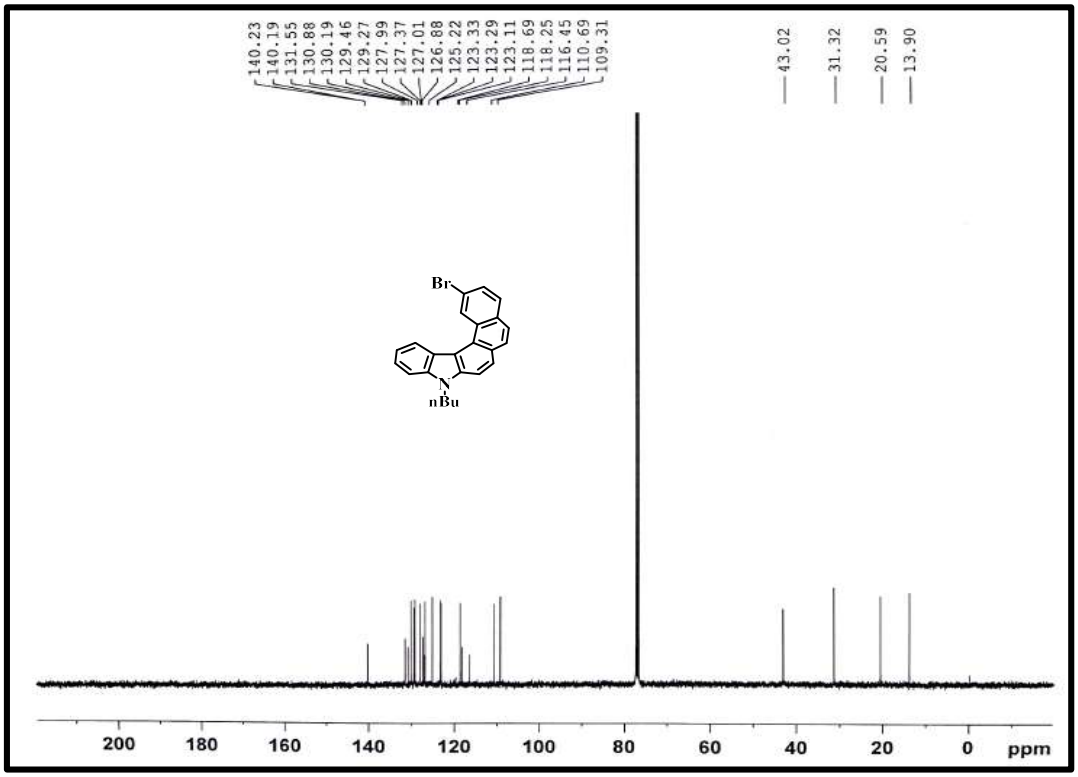

[13]C NMR spectra of compound 32

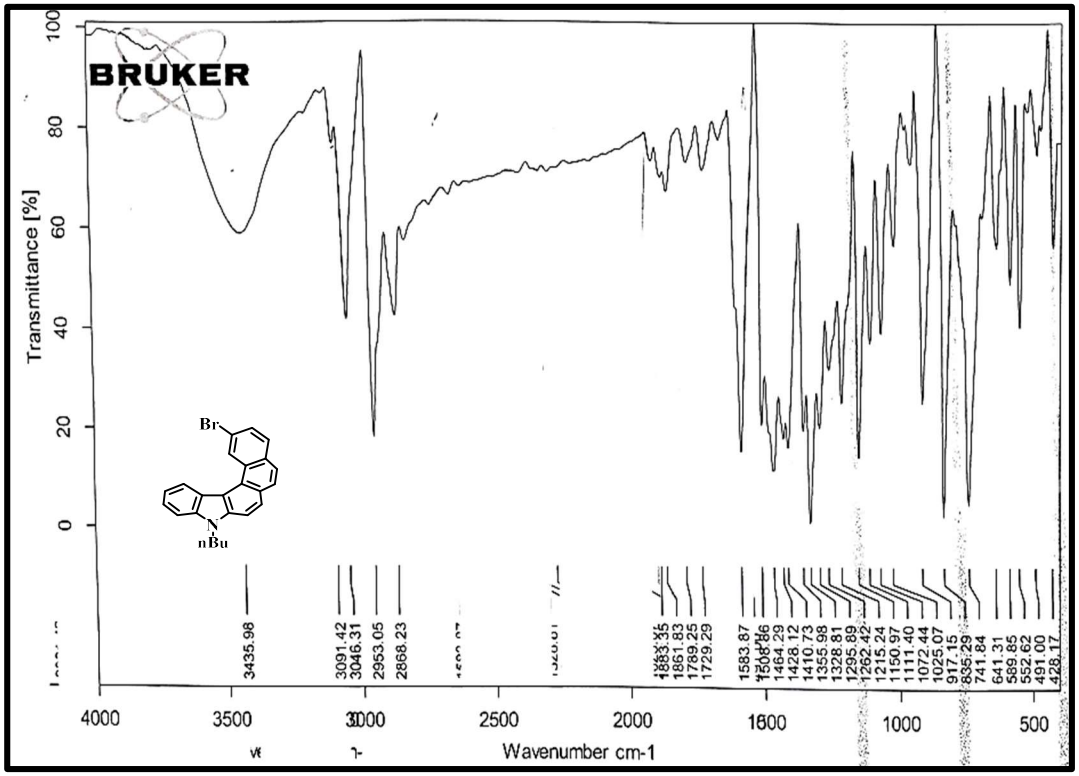

IR spectra of compound 32

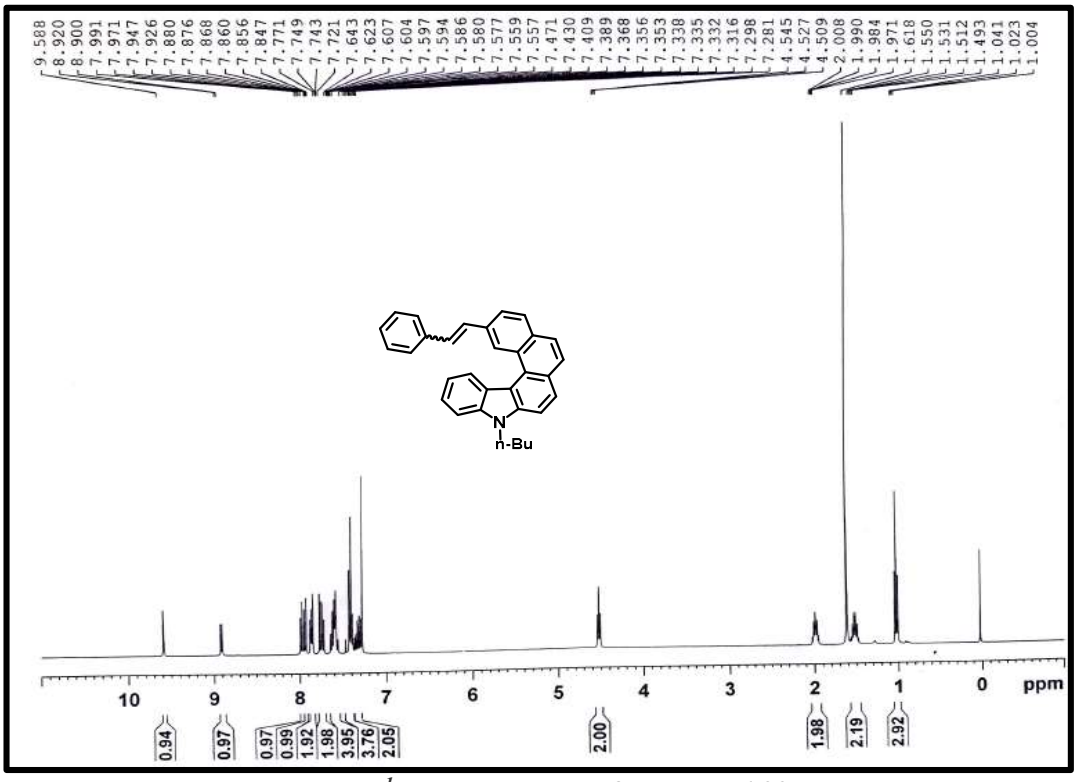

^{1}H NMR spectra of compound 33

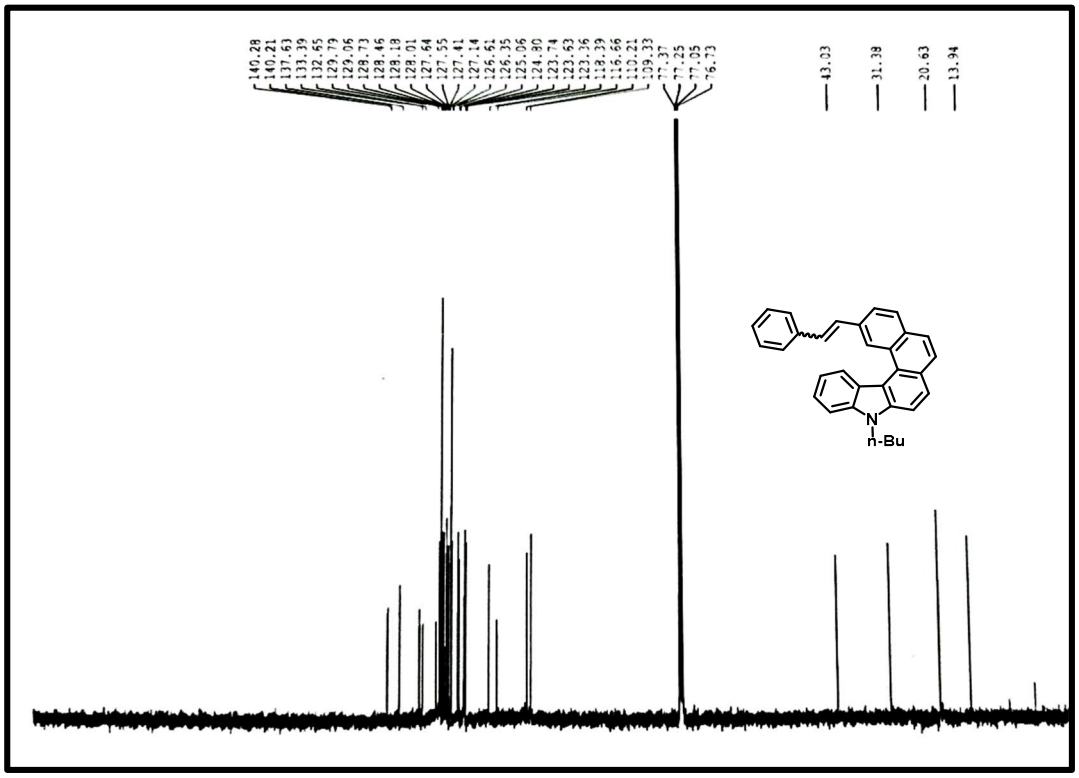

^{13}C NMR spectra of compound 33

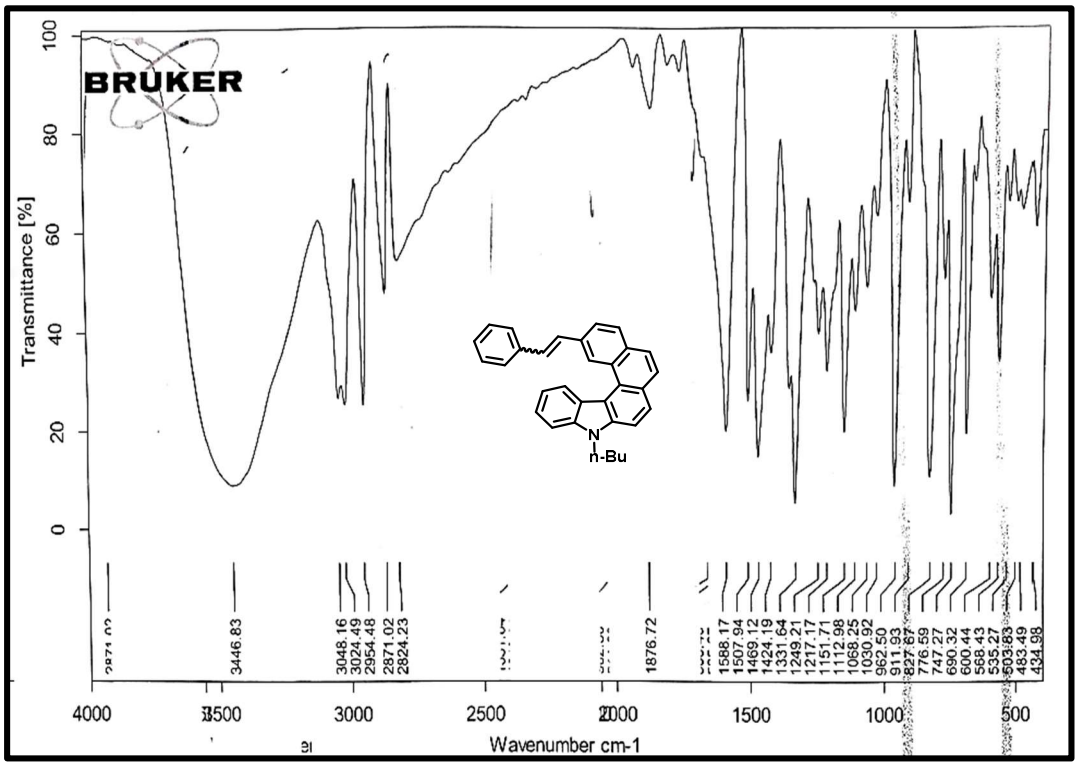

IR spectra of compound 33

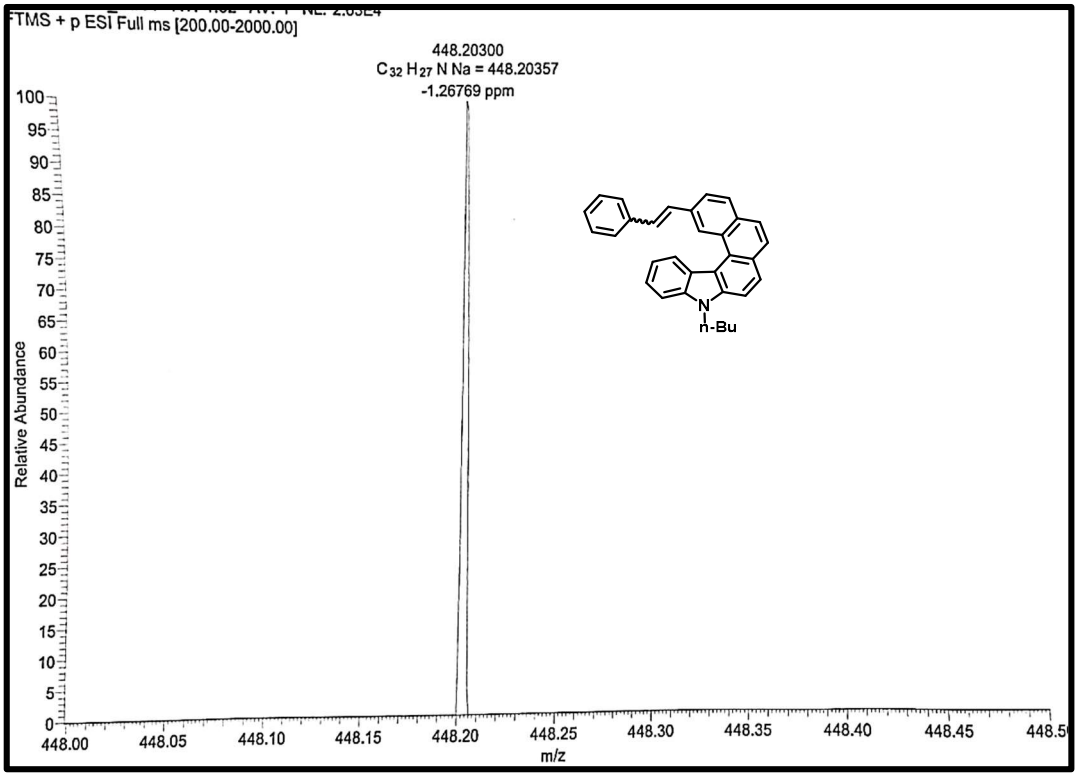

HRMS spectra of compound 33

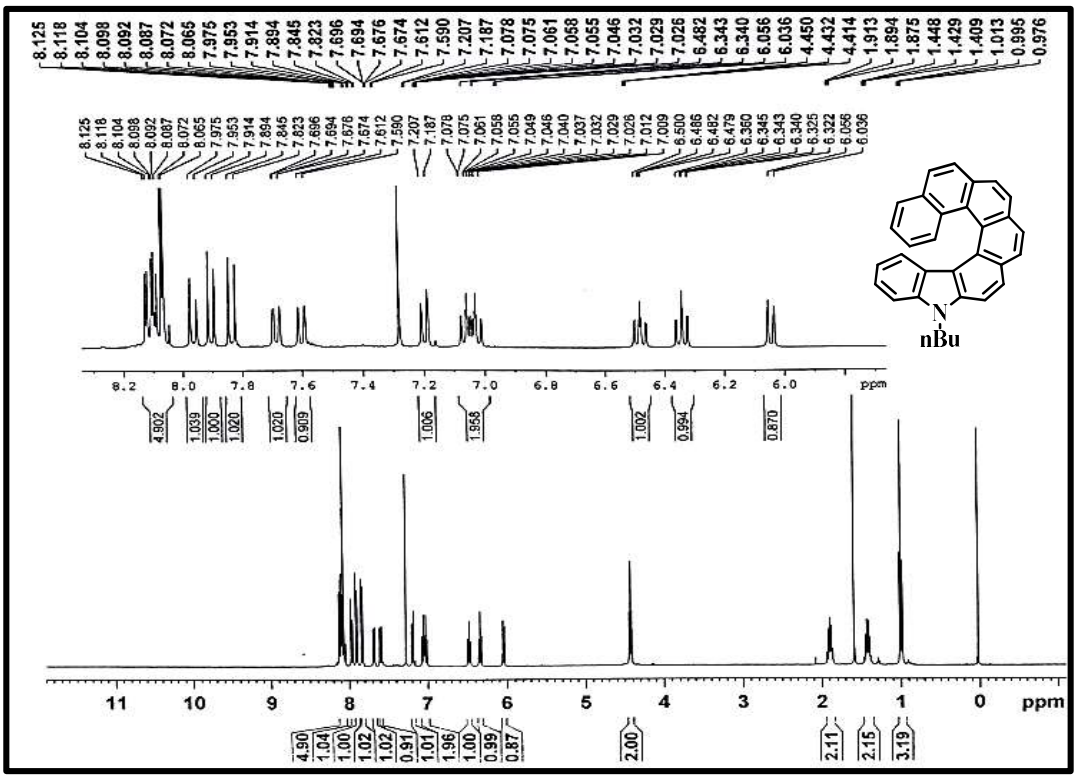

^{1}H-NMR spectra of compound 34

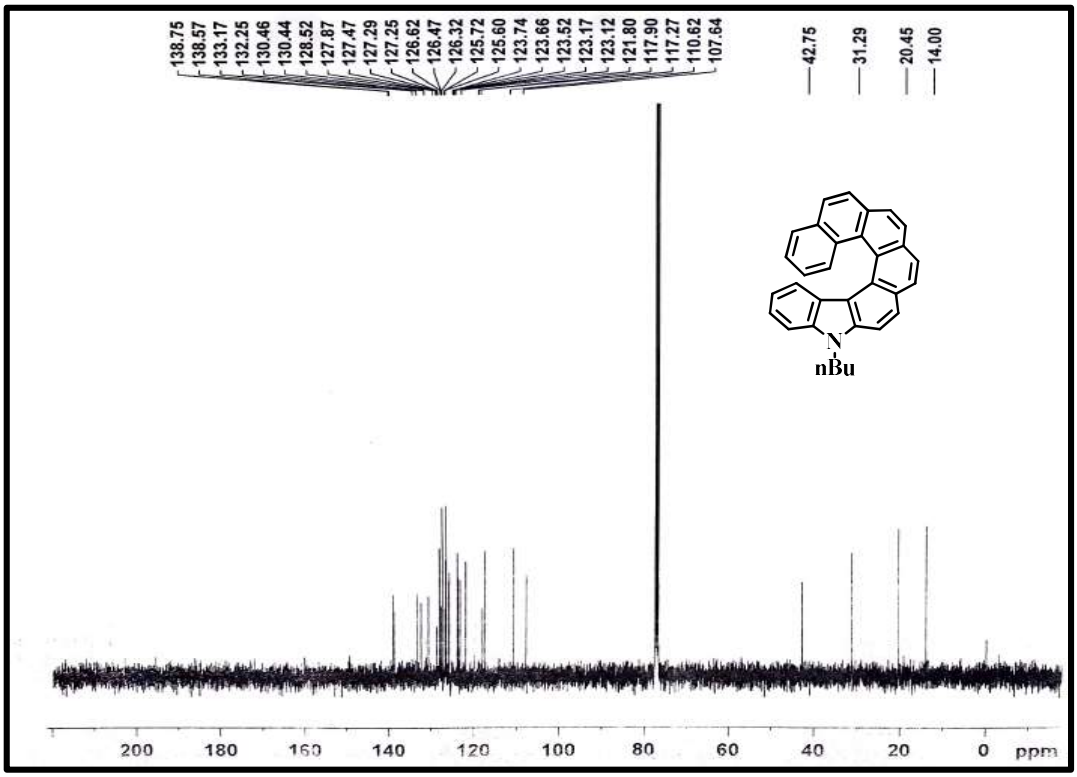

^{13}C-NMR spectra of compound 34

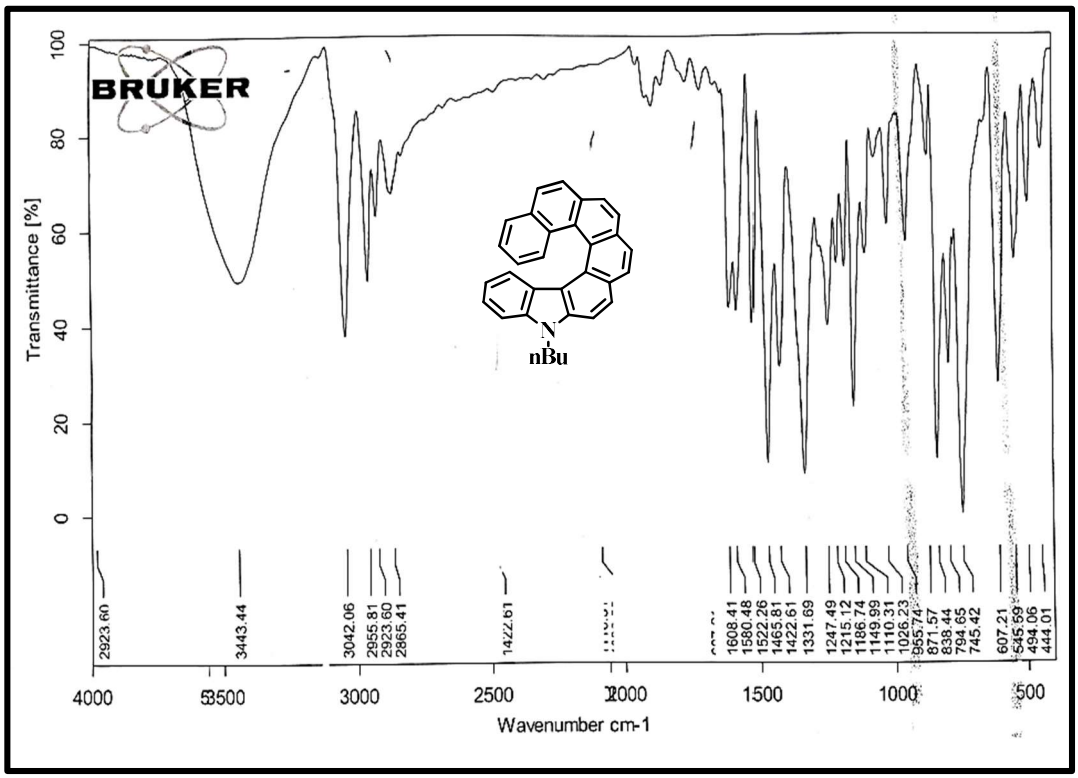

IR spectra of compound 34

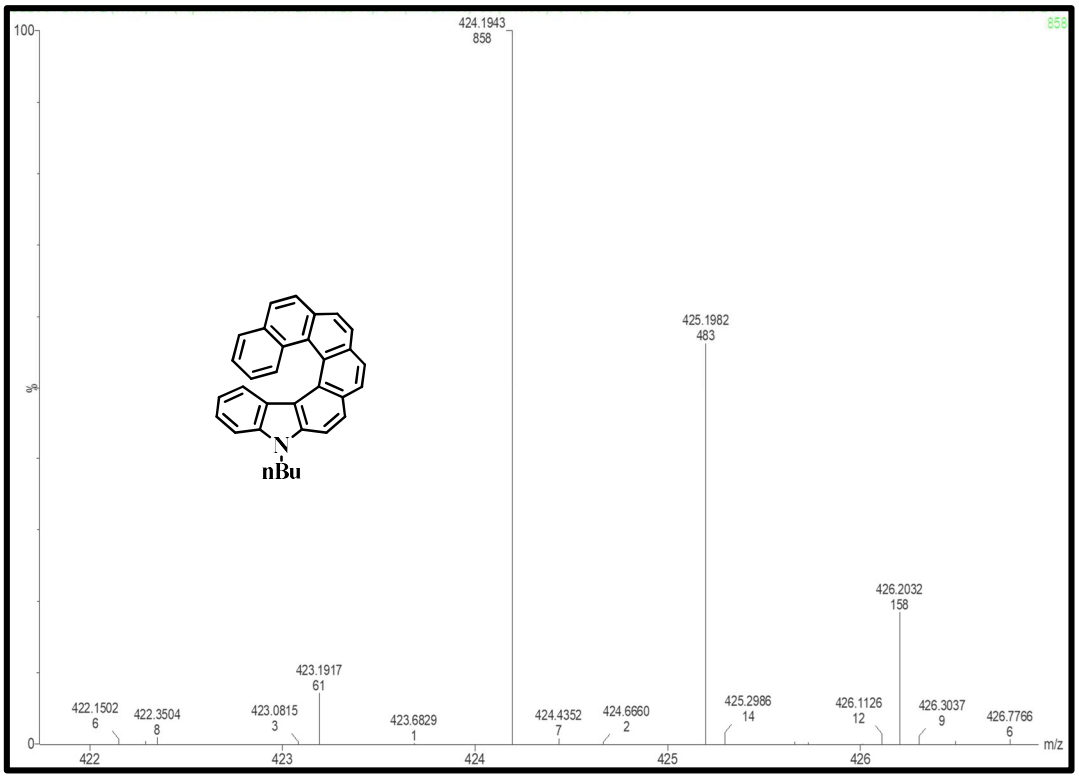

HRMS spectra of compound 34

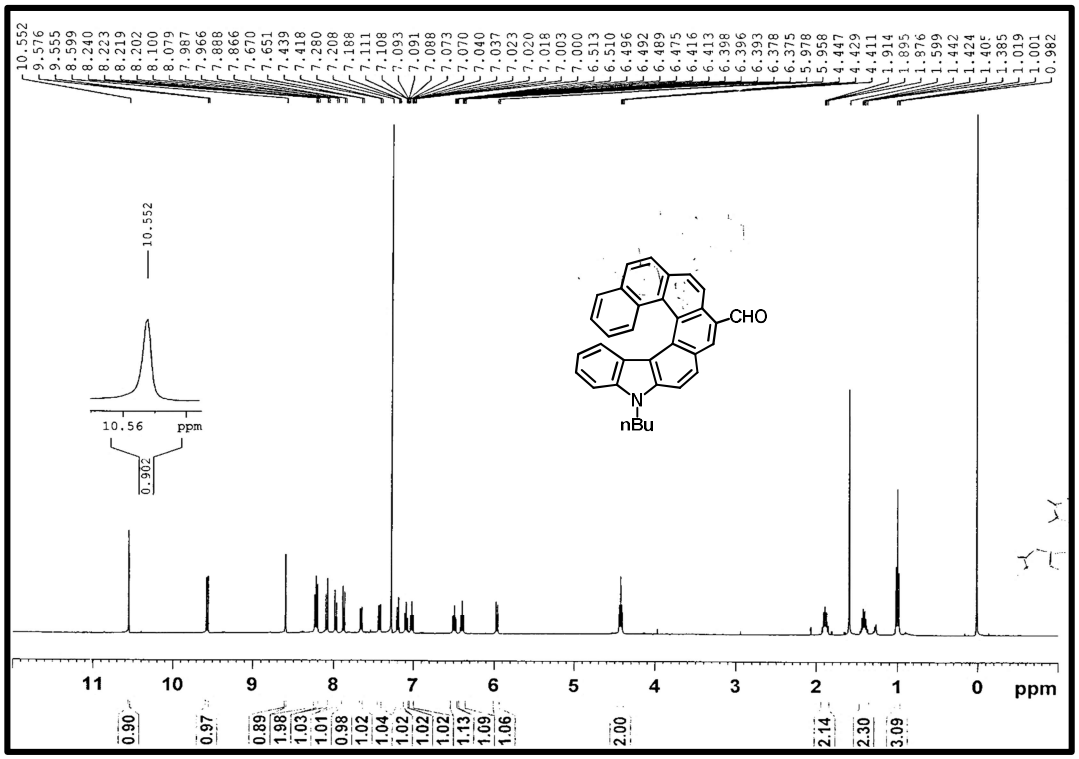

^{1}H-NMR spectra of compound 36b

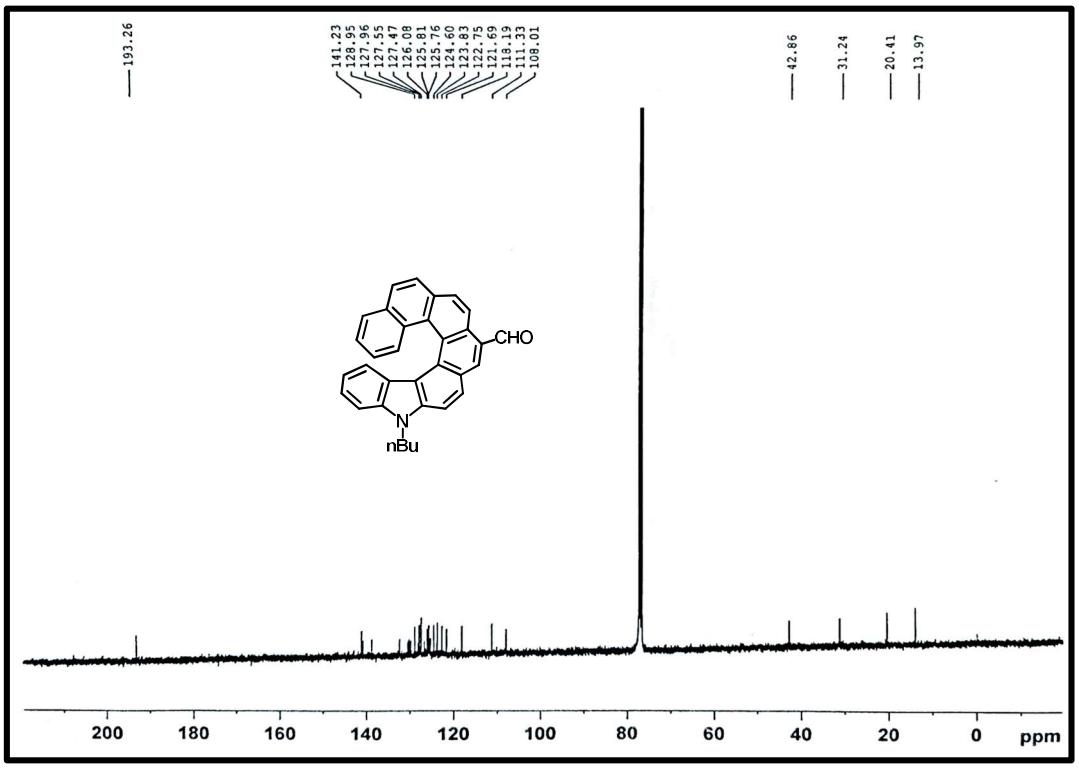

^{13}C NMR spectrum of compound 36

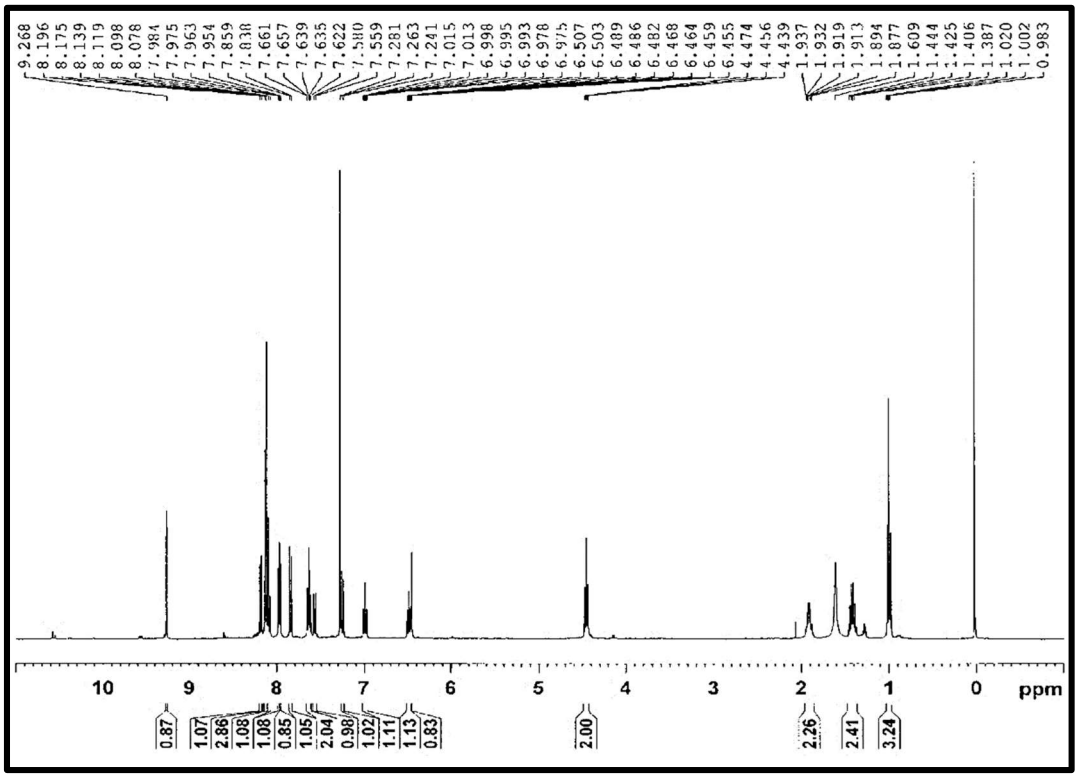

^{1}H-NMR spectrum of compound 36a

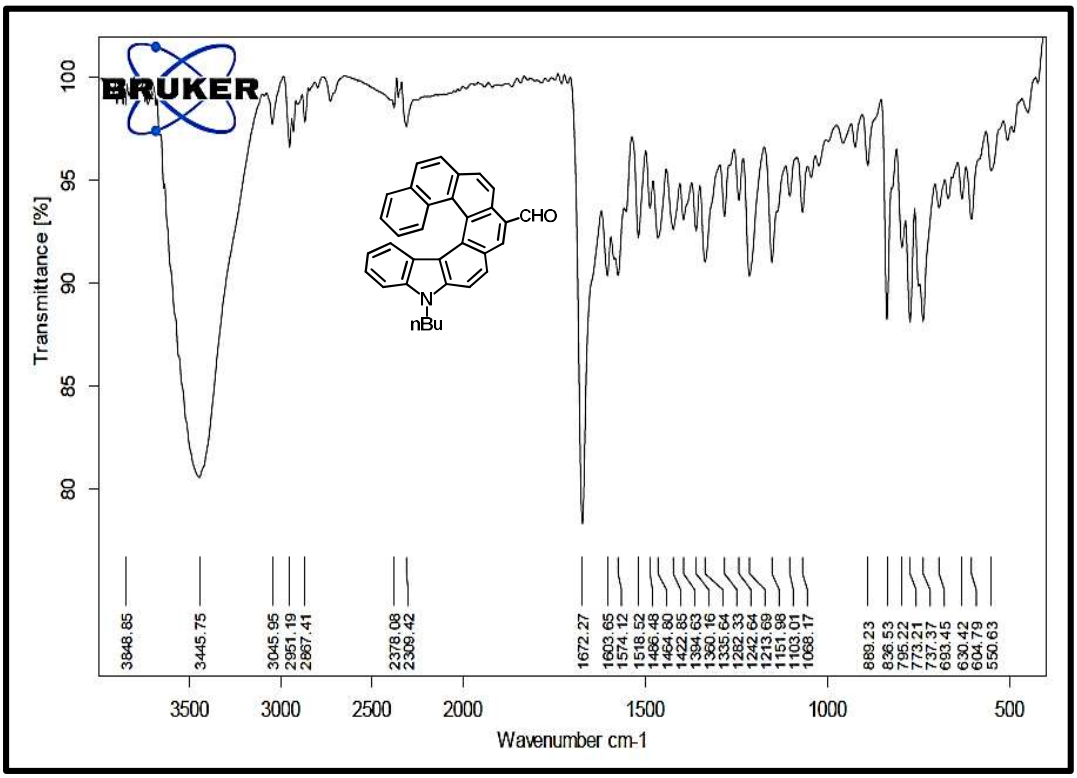

IR spectra of compound 36

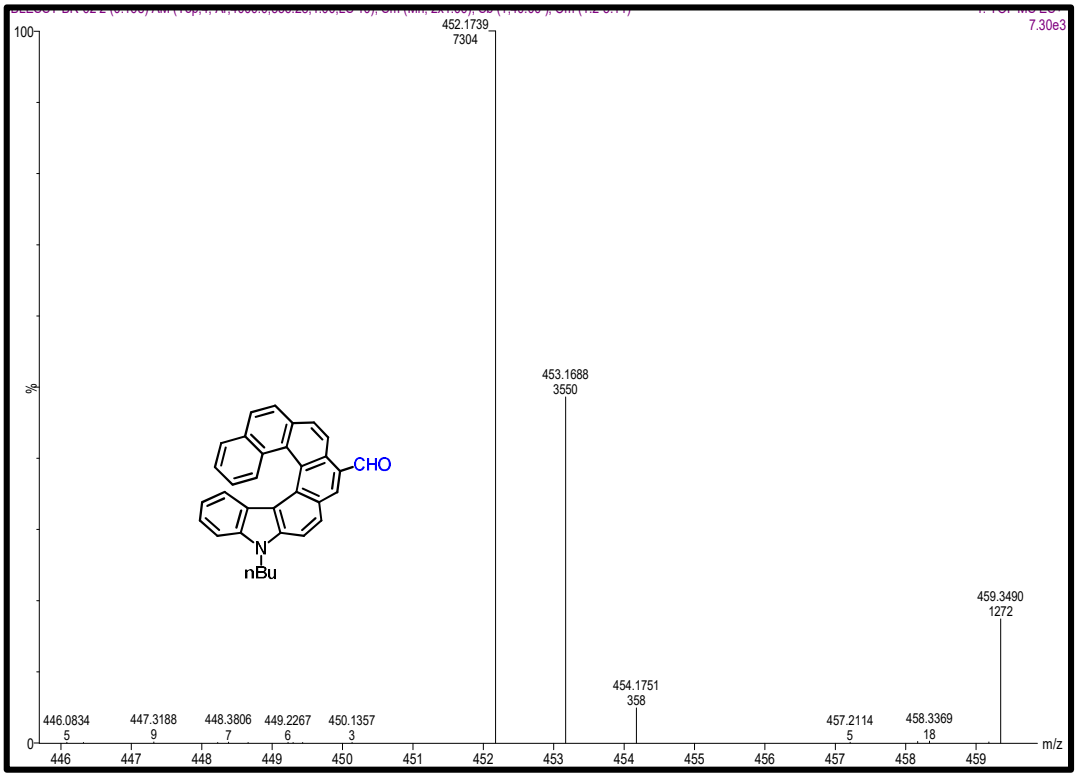

HRMS spectra of compound 36

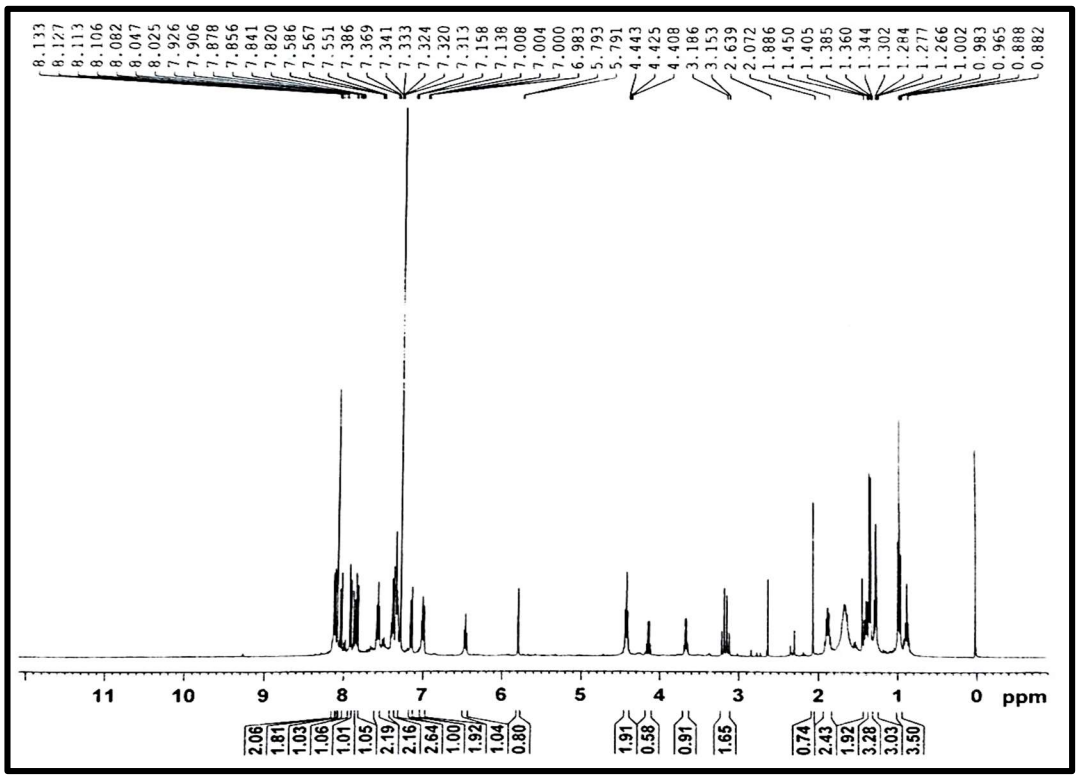

[1]H-NMR spectra of compound 37

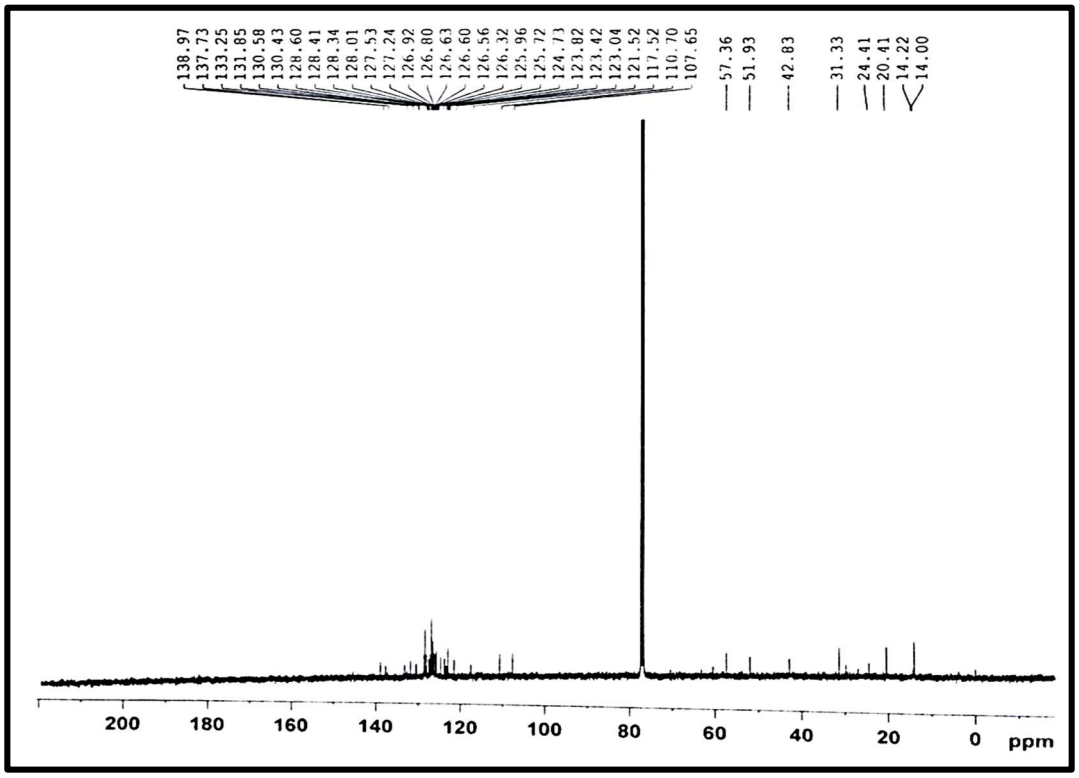

[13]C NMR spectrum of compound 37

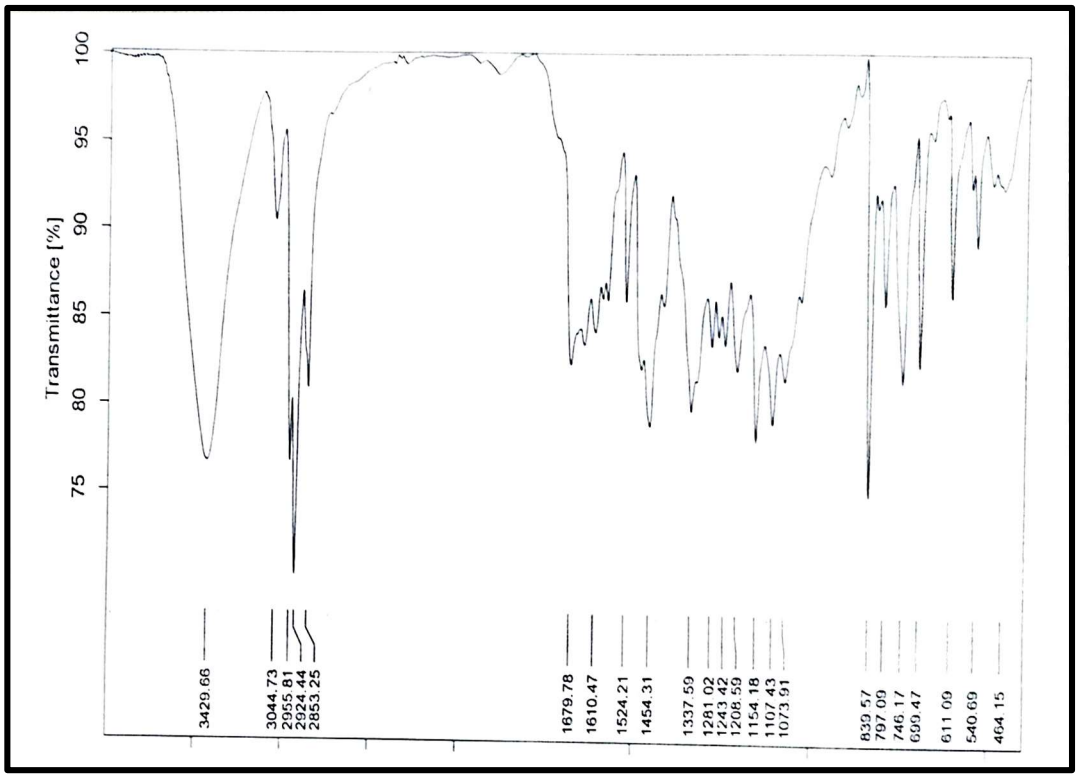

IR spectrum of compound 37

	No.	Sample No	Mode	Measurement Date	Monitor(deg)	Calc. Data	Temperature(C)
1 *	1	br a2-1	Specific O.R.	8/25/2021 5:33 PM	-0.5349	-5349.0000	29.86
2 *	2	br a2-2	Specific O.R.	8/25/2021 5:33 PM	-0.5350	-5350.0000	29.86
3 *	3	br a2-3	Specific O.R.	8/25/2021 5:33 PM	-0.5358	-5358.0000	29.86
4 *	4	Avg.				-5352.3333	
5	5	S.D				4.9329	
6	6	C.V				0.0922	

Specific optical rotation data of compound 37 with concentration of 0.1 w/v in 10mm pathlength polarimeter cell

3.1.8 References

1. Fox, J. M. & Katz, T. J. Conversion of a [6]Helicene into an [8]Helicene and a Helical 1,10-Phenanthroline Ligand. *The Journal of Organic Chemistry* **64**, 302-305 (1999).
2. Schneider, J. F., Nieger, M., Nättinen, K., Lewall B. Novel [6]- and [7]Helicene-like quinones via mono- and bidirectional chromium templated benzannulation of bridged binaphthyl carbene complexes. *European Journal of Organic Chemistry* **8,** 1541-1560 (2005).
3. Schneider, J. F., Nieger, M., Nättinen, K. & Dötz, K. H. A novel approach to functionalized heterohelicenes via chromium-templated benzannulation reactions. *Synthesis* **7**, 1109–1124 (2005).
4. Shyam Sundar, M., Bedekar, A. V. Synthesis and Study of 7,12,17-Trioxa[11]helicene. *Organic Letters* **17**, 5808–5811 (2015).
5. Hua, W., Z. Liu, L. Duan, G. Dong, Y. Qiu, B. Zhang, D. Cui, X. Tao, N. Cheng, Y. Liu, Deep-blue electroluminescence from nondoped and doped organic light-emitting diodes (OLEDs) based on a new monoaza[6]helicene. *RSC Advances* **5**, 75–84 (2015).
6. Ben Braiek, M., Aloui, F., Moussa, S., Ben Hassine B. Synthesis, X-ray analysis and photophysical properties of a new *N*-containing pentacyclic helicene. *Tetrahedron Letters* **54**, 5421–5425 (2013).
7. Weix, D.J., Dreher, S.D., Katz, T.J., [5]HELOL phosphite: A helically grooved sensor of remote chirality. *Journal of American Chemical Society* ***122***, 10027–10032 (2000).
8. Wang, D.Z.G., Katz, T.J. A [5]HELOL analogue that senses remote chirality in alcohols, phenols, amines, and carboxylic acids. *The Journal of Organic Chemistry*, ***70***, 8497–8502 (2005).
9. Li Y-Y, Lu H-Y, Li M, Li X-J, Chen C-F, Dihydroindeno[2,1-*c*]fluorene-based imide dyes: Synthesis, structures, photophysical and electrochemical properties. *The Journal of Organic Chemistry* ***79***, 2139–2147 (2014).

10. Narcis, M. J., Takenaka, N. Helical chiral small molecules in asymmetric catalysis *European Journal of Organic Chemistry*, ***2014***, 21–34 (2014).

11. Anger, E., Iida, H., Yamaguchi, T., Hayashi, K., Kumano, D., Crassous, J., Vanthuyne, N., Roussel, C., Yashima, E. Synthesis and chiral recognition ability of helical polyacetylenes bearing helicene pendants. *Polymer Chemistry*, ***5*,** 4909-4914 (2014)

12. (a) Jhulki, S., Mishra, A. K., Chow, T. J., Moorthy, J. N. Helicenes as all in one organic materials….aza[5]helical diamines. *Chemistry - A European Journal* ***22***, 9375–9386 (2016). (b) Shi, L., Liu, Z., Dong, G., Duan, L., Qiu, Y., Jia, J., Guo, W., Zhao, D., Cui, D., Tao, X. Synthesis, structure, properties, and application of carbazole-based...OLED. *Chemistry - A European Journal*, ***18***, 8092–8099 (2012).

13. Hu, J-Y., Paudel, A., Seto, N., Feng, X., Era, M., Matsumoto, T., Tanaka, J., Elsegood, M.R.J., Redshaw, C., Yamato, T., Pyrene-cored blue light emitting...properties. *Organic and Biomolecular Chemistey*, ***11***, 2186–2197 (2013).

14. Shen, Y., Chen, C-F. Helicenes: synthesis and applications *Chemical Rev*iews, ***112***, 1463–1535 (2012).

15. Teply F, Stara IG, Stary I, Kollarovic A, Saman D, Rulisek L, Fiedler P, *J Am Chem Soc*, ***124*,** 9175–9180 (2002).

16. (a) T. Yamamoto, Y. Akai, Y. Nagata, M. Suginome, *Angewandte Chemie - International Edition*, ***50***, 8844–8847 (2011). (b) J. Misek, F. Teply, I. G. Stara, M. Tichy, D. Saman, I. Cisarova, P. Vojtisek, I. A. Stary, *Angew. Chem. Int. Ed.*, ***47*,** 3188–3191 (2008).

18. X. Zhou, J. He, L. S. Liao, M. Lu, X. M. Ding, X. Y. Hou, X. M. Zhang, X. Q. He, S. T. Lee, *Adv. Mater.*, ***12*,** 265–269 (2000).